

Unraveling the dynamics of the Omicron and Delta variants of the 2019 coronavirus in the presence of vaccination, mask usage, and antiviral treatment

Calistus N. Ngonghala^{a,b,*}, Hemaho B. Taboe^{a,c}, Salman Safdar^d, Abba B. Gumel^{d,e}

^aDepartment of Mathematics, University of Florida, Gainesville, FL 32611, USA.

^bEmerging Pathogens Institute, University of Florida, Gainesville, FL 32610, USA.

^cLaboratoire de Biomathématiques et d'Estimations Forestières, University of Abomey-Calavi, Cotonou, Bénin.

^dSchool of Mathematical and Statistical Sciences, Arizona State University, Tempe, Arizona, 85287, USA.

^eDepartment of Mathematics and Applied Mathematics, University of Pretoria, Pretoria 0002, South Africa.

Abstract

The effectiveness of control interventions against COVID-19 is threatened by the emergence of SARS-CoV-2 variants of concern. We present a mathematical model for studying the transmission dynamics of two of these variants (Delta and Omicron) in the United States, in the presence of vaccination, treatment of individuals with clinical symptoms of the disease and the use of face masks. The model is parameterized and cross-validated using observed daily case data for COVID-19 in the United States for the period from November 2021 (when Omicron first emerged) to March 2022. Rigorous qualitative analysis of the model shows that the disease-free equilibrium of the model is locally-asymptotically stable when the control reproduction number of the model (denoted by \mathbb{R}_c) is less than one. This equilibrium is shown to be globally-asymptotically stable for a special case of the model, where disease-induced mortality is negligible and both vaccine-derived immunity in fully-vaccinated individuals and natural immunity do not wane, when the associated reproduction number is less than one. The epidemiological implication of the latter result is that the combined vaccination-boosting strategy can lead to the elimination of the pandemic if its implementation can bring (and maintain) the associated reproduction number to a value less than one. An analytical expression for the vaccine-derived herd immunity threshold is derived. Using this expression, together with the baseline values of the parameters of the parameterized model, we showed that the vaccine-derived herd immunity can be achieved in the United States (so that the pandemic will be eliminated) if at least 68% of the population is fully-vaccinated with two of the three vaccines approved for use in the United States (Pfizer or Moderna vaccine). Furthermore, this study showed (as of the time of writing in March 2022) that the control reproduction number of the Omicron variant was approximately 3.5 times that of the Delta variant (the reproduction of the latter is computed to be ≈ 0.2782), indicating that Delta had practically died out and that Omicron has competitively-excluded Delta (to become the predominant variant in the United States). Based on our analysis and parameterization at the time of writing of this paper (March 2022), our study suggests that SARS-CoV-2 elimination is feasible by June 2022 if the current baseline level of the coverage of fully-vaccinated individuals is increased by about 20%. The prospect of pandemic elimination is significantly improved if vaccination is combined with a face mask strategy that prioritizes moderately effective and high-quality masks. Having a high percentage of the populace wearing the moderately-effective surgical mask is more beneficial to the community than having low percentage of the populace wearing the highly-effective N95 masks. We showed that waning natural and vaccine-derived immunity (if considered individually) offer marginal impact on disease burden, except for the case when they wane at a much faster rate (e.g., within three months), in comparison to the baseline (estimated to be within 9 months to a year). Treatment of symptomatic individuals has marginal effect in reducing daily cases of SARS-CoV-2, in comparison to the baseline, but it has significant impact in reducing daily hospitalizations. Furthermore, while treatment significantly reduces daily hospitalizations (and, consequently, deaths), the prospects of COVID-19 elimination in the United States are significantly enhanced if investments in control resources are focused on mask usage and vaccination rather than on treatment.

Keywords: COVID-19; vaccination; antiviral treatment; masks, reproduction number; waning immunity; vaccine-derived herd immunity.

1. Introduction

The 2019 novel coronavirus (COVID-19), caused by SARS-CoV-2, resulted in an unprecedented pandemic never before seen since the 1918 influenza pandemic [1–5]. As of February 22, 2022, the SARS-CoV-2 pandemic had caused over 427.8 million confirmed cases and 5.9 million deaths globally [6, 7]. The rapid development and deployment of effective vaccines has played a major role in minimizing and mitigating the burden of the pandemic in regions with moderate and high vaccination coverage [8–10]. Specifically, as of February 11, 2022, 27 vaccines had been approved for use in numerous countries around the world [11]. Three of these vaccines, developed by Pfizer/BioNTech, Moderna and Johnson & Johnson, have been approved by the United States Food and Drugs Administration (FDA) [12, 13]. The Pfizer and

20 Moderna vaccines are designed by introducing messenger ribonucleic acid (mRNA) that encodes the spike protein of
21 SARS-CoV-2 to elicit an adaptive immune response against the disease [14]. These vaccines, which are primarily ad-
22 ministered in a two-dose regimen three to four weeks apart, have an estimated protective efficacy against symptomatic
23 COVID-19 infection of 95% [15–17]. A third (booster) dose was approved for these vaccines on November 19, 2021 for
24 all adults from 18 years old [18]. The Johnson and Johnson vaccine, on the other hand, was developed using adenovirus
25 vector encoding the SARS-CoV-2 spike protein, and is administered in a single dose regimen. Its efficacy against mod-
26 erate to severe infection is estimated to be 67% [19]. We focus on two of the three vaccines used in the United States.

27 Despite the deployment of the three safe and effective vaccines in the United States (since late 2020 to early 2021), SARS-
28 CoV-2 transmission in the United States is still on the rise (see, for example, Figure 1). Specifically, as of the time of writing
29 (mid-February 2022), the United States is recording a 7-days average of 172,951 new COVID-19 cases *per day* [6]. This
30 is largely due to vaccine hesitancy or refusal (only about 64% of the population in the United States is fully-vaccinated;
31 with 43% of this population having received the booster dose as of February 14, 2022) and the emergence of new SARS-
32 CoV-2 variants [20–25]. Thus, the approved vaccines, despite their high efficacy against the original SARS-CoV-2 strain,
33 are currently insufficient to halt the COVID-19 pandemic in the United States. Hence, other control measures, such
34 as antivirals that reduce the risk of disease progression, are needed to add to the armoury of measures for effectively
35 combating or eliminating the COVID-19 pandemic in the United States. It is worth stating that the phenomenon of vac-
36 cine hesitancy or refusal during outbreaks of highly contagious and/or fatal vaccine-preventable infectious diseases of
37 humans has a long history, dating back to the 1800s [26–30]. That is, vaccine hesitancy, refusal or general controversy
38 surrounding vaccination programs in humans did not just start with the COVID-19 pandemic.

39 Two antiviral drugs, namely, *Paxlovid* (developed by Pfizer Inc.) and *Molnupiravir* (developed by Merck Inc.), received
40 FDA-Emergency Use Authorization in December 2021, for healthcare providers to use to treat mild-to-moderate COVID-
41 19 in adults and pediatric patients (12 years of age and older weighing at least 40 kg) [31]. These antivirals primarily work
42 by altering the genetic code of SARS-CoV-2 and inhibiting it from replicating. Paxlovid, which is administered as three
43 tablets taken together orally twice daily for five days, is estimated to reduce the risk of hospitalization or death by 90%
44 [32]. Molnupiravir, which is administered as four 200 milligram capsules taken orally every 12 hours for five days, is
45 effective in reducing hospitalization or death by 31% [33]. Full efficacy of these antivirals is achieved if used during the
46 first five days of onset of symptoms [33, 34].

47 The unprecedented level of community transmission of SARS-CoV-2 in the United States has resulted in the emergence
48 of numerous mutants (variants of concern) [35–40]. The Delta variant (B.1.617.2), which was first identified in India in
49 late 2020 [41], emerged in the United States in July 27, 2021. This variant, which was believed to be more than twice as
50 contagious as previous SARS-CoV-2 variants, quickly spread across the United States causing unprecedented levels of
51 hospitalizations and deaths. It remained the dominant variant (accounting for 99% of all new cases) until mid-December
52 2021 (see the region between the dashed green and purple vertical lines in Figure 1), when a new variant (Omicron;
53 B.1.1.529) emerged [37]. Omicron, believed to be three times more contagious than Delta, quickly displaced Delta, and
54 became the predominant variant [17, 42, 43] (see regions to the right of the dashed purple vertical line in Figure 1).

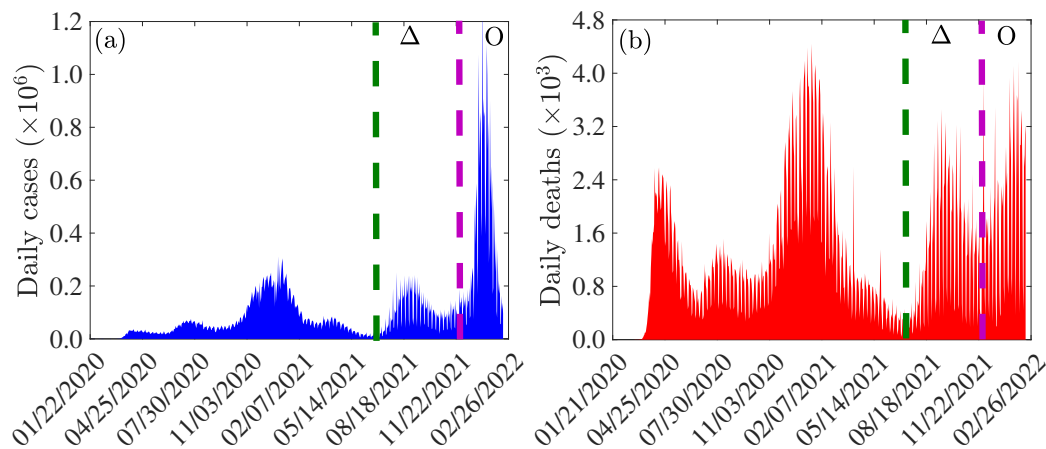


Fig. 1: Data for COVID-19 daily (a) cases and (b) mortality for the United States for the period of the COVID-19 pandemic from January 2020 to February 2022. The data is obtained from the Johns Hopkins University COVID-19 Dashboard [7, 44]. The burden of the Delta variant is in the regions between the green and purple dashed vertical lines (denoted by Δ), while that of the Omicron variant is in the region to the right of the dashed purple vertical line (denoted by O).

55 The three FDA-approved vaccines used in the United States were designed against the original SARS-Cov-2 strain, and
 56 only offer cross-protective efficacy against the variants [14, 17, 45]. It is, therefore, instructive to theoretically assess,
 57 through mathematical modeling and analysis, the population-level effectiveness of the vaccines against the two remain-
 58 ing dominant variants (namely, Delta and the current predominant, Omicron). The current study is based on the design
 59 of a mathematical model for assessing the qualitative dynamics of the two dominant SARS-CoV-2 variants co-circulating
 60 in the United States (Delta and Omicron). The resulting two-strain model, which takes the form of a deterministic system
 61 of nonlinear differential equations, incorporates treatment of individuals with clinical symptoms of SARS-CoV-2 (using
 62 the two FDA-EUA antivirals discussed above). The model is formulated in Section 2.1 and fitted using daily case data for
 63 COVID-19 in the United States for the period when Omicron first appeared in the country (i.e., from November 28, 2021
 64 to January 31, 2022), as well as cross-validated using the portion of the daily case data from February 1, 2022 to March 18,
 65 2022 and cumulative case data for COVID-19 in the United States (for the period from November 28, 2021 to March 18,
 66 2022) in Section 2.2. Basic theoretical results, for the existence and asymptotic stability of the disease-free equilibrium
 67 of the model, are provided in Section 3. Furthermore, the condition, in parameter space, for achieving vaccine-derived
 68 herd immunity is derived. Numerical simulations are presented in Section 4 and a discussion of the results and con-
 69 cluding remarks are presented in Section 5. It should be mentioned that this study was conducted between November
 70 2021 to March 2022 (and the reader should interpret our results bearing this context and fact in mind).

71 2. Methods

72 2.1. Formulation of Mathematical Model

73 The mathematical model to be developed in this study is for the transmission dynamics of the COVID-19 pandemic in
 74 the United States for the scenario where the dominant variant of concern was initially Delta and the new prevailing and
 75 currently dominant variant, Omicron, is introduced (this was the scenario in the United States when Omicron emerged
 76 in the Fall of 2021). Let $N(t)$ denote the total population of the United States at time t . This population is stratified into
 77 the mutually-exclusive compartments for unvaccinated susceptible ($S(t)$), fully-vaccinated but not boosted susceptible
 78 ($V_f(t)$; these are individuals that have either received the two doses of the FDA-approved Pfizer or Moderna vaccine or
 79 the single dose of Johnson & Johnson vaccine), fully-vaccinated and boosted susceptible ($V_b(t)$), exposed/latent ($E_j(t)$),
 80 presymptomatic ($P_j(t)$), detected infected individuals from the exposed, presymptomatic, and asymptomatic classes
 81 ($Q_j(t)$), symptomatic infectious within the first five days of onset of symptoms ($I_{j1}(t)$), symptomatic individuals af-
 82 ter the first five days of onset of symptoms ($I_{j2}(t)$), asymptomatic infectious or symptomatic infectious with very mild
 83 symptoms ($A_j(t)$), hospitalized ($H_j(t)$) and recovered ($R_j(t)$) individuals, so that (where we used the subscript notation
 84 $j \in \{d, o\}$, with d and o representing the Delta and Omicron variant, respectively):

$$N(t) = S(t) + V_f(t) + V_b(t) + \sum_{j=d,o} [E_j(t) + P_j(t) + Q_j(t) + I_{j1}(t) + I_{j2}(t) + A_j(t) + H_j(t) + R_j(t)]. \quad (2.1)$$

85 The population of unvaccinated susceptible individuals is increased by recruitment into the population at a rate Λ and
 86 by the waning of vaccine-derived protective immunity in fully-vaccinated but not boosted (at a rate ω_{vf}) and fully-
 87 vaccinated and boosted (at a rate ω_{vb}) individuals. It is further increased by the loss of natural immunity in individuals
 88 who recovered from Delta (at a rate ω_{dr}) and Omicron (at a rate ω_{or}) infection. Unvaccinated susceptible individuals are
 89 fully-vaccinated (but not boosted) at a rate ξ_{vf} . Individuals in all epidemiological compartments suffer natural death at
 90 a rate μ . Unvaccinated susceptible individuals acquire infection with the Delta variant at a rate λ_d and with Omicron at
 91 a rate λ_o , where:

$$\lambda_d = \frac{\beta_{dp}P_d + \beta_{da}A_d + \beta_{dq}Q_d + \beta_{d1}I_{d1} + \beta_{d2}I_{d2} + \beta_{dh}H_d}{N}, \quad (2.2)$$

92 and,

$$\lambda_o = \frac{\beta_{op}P_o + \beta_{oa}A_o + \beta_{oq}Q_o + \beta_{o1}I_{o1} + \beta_{o2}I_{o2} + \beta_{oh}H_o}{N}. \quad (2.3)$$

93 In (2.2)–(2.3), β_{jp} , β_{ja} , β_{jq} , β_{ji} and β_{jh} (with $j = d, o, i = 1, 2$) represent, respectively, the transmission rate by presymp-
 94 tomatic, asymptomatic, detected, symptomatic, and hospitalized infectious individuals. It should be mentioned that
 95 detected individuals are supposed to be isolated (or removed) from the actively-mixing population. However, in reality,
 96 isolation is not always perfectly implemented (leading to the well-known notion of *leaky isolation*, where some isolated
 97 individuals escape isolation for all sorts of reasons, such as economics (to allow them go to work; particularly those
 98 who live from paycheck-to-paycheck) or human behavior change, leading them to choose to opt out of the isolation
 99 protocols). Our modeling allows for the possibility that not all detected individuals will strictly adhere to the isolation

100 protocols (so that some level of disease transmission can occur by detected individuals who are supposed to be “iso-
 101 lated”). This is reflected in our parameter estimation in Section 2.2, where the estimated value for the transmission rates
 102 for detected individuals are very small, compared to those for infectious individuals who are not in isolation (see Table
 103 S4 of the Supplementary Information). Furthermore, it should be noted that individuals entering the Q_j class from the E
 104 class are infected but not (yet) infectious. In other words, not all individuals in the Q_j class are infectious. We account for
 105 this fact by re-defining the effective contact rate for individuals in the Q_j class ($\beta_{jq}, j = d, o$) as $\beta_{jq} = q_1 \tilde{\beta}_{jq}$, where $\tilde{\beta}_{jq}$
 106 is the overall effective contact rate for individuals in the Q_j class and $0 < q_1 \leq 1$ is a modification parameter accounting
 107 for the proportion of individuals in the Q_j class who are actually infectious.

108 Fully-vaccinated (but not boosted) individuals acquire breakthrough infection with Delta (at a rate λ_{df}) or Omicron (at
 109 a rate λ_{of}), where:

$$\lambda_{df} = (1 - \varepsilon_{df}) \frac{\beta_{dp}P_d + \beta_{da}A_d + \beta_{dq}Q_d + \beta_{d1}I_{d1} + \beta_{d2}I_{d2} + \beta_{dh}H_d}{N}, \quad (2.4)$$

110 and,

$$\lambda_{of} = (1 - \varepsilon_{of}) \frac{\beta_{op}P_o + \beta_{oa}A_o + \beta_{oq}Q_o + \beta_{o1}I_{o1} + \beta_{o2}I_{o2} + \beta_{oh}H_o}{N}, \quad (2.5)$$

111 with $0 < \varepsilon_{jf} < 1$ representing the cross-protective efficacy the vaccine offers against Delta (ε_{df}) or Omicron (ε_{of}) variant.
 112 Fully-vaccinated individuals receive the booster dose (at a rate rate ξ_{vb}) and lose their vaccine-derived immunity (at a
 113 rate ω_{vf}). Vaccinated individuals who received the booster dose acquire infection with Delta (at a rate λ_{db}) or Omicron
 114 (at a rate λ_{ob}), where:

$$\lambda_{db} = (1 - \varepsilon_{db}) \frac{\beta_{dp}P_d + \beta_{da}A_d + \beta_{dq}Q_d + \beta_{d1}I_{d1} + \beta_{d2}I_{d2} + \beta_{dh}H_d}{N}, \quad (2.6)$$

115 and,

$$\lambda_{ob} = (1 - \varepsilon_{ob}) \frac{\beta_{op}P_o + \beta_{oa}A_o + \beta_{oq}Q_o + \beta_{o1}I_{o1} + \beta_{o2}I_{o2} + \beta_{oh}H_o}{N}, \quad (2.7)$$

116 with $0 < \varepsilon_{db} < 1$ and $0 < \varepsilon_{ob} < 1$ representing the cross-protective efficacy the vaccine offers boosted individuals against
 117 Delta and Omicron, respectively. Exposed (or latent) individuals progress to the pre-symptomatic class at a rate σ_{je} .
 118 Furthermore, individuals in the pre-symptomatic class progress, at the end of the incubation period, to either the symp-
 119 tomatic class (at a rate $r_j \sigma_{jp}$; where $0 < r_j < 1$ is the proportion of these individuals that display clinical symptoms of
 120 SARS-CoV-2 at the end of the incubation period) or the asymptomatic infectious class (at a rate $(1 - r_j) \sigma_{jp}$). Asymp-
 121 tomatic infectious individuals recover (naturally) at a rate γ_{ja} . Infected individuals in the exposed, presymptomatic
 122 and asymptomatic classes are detected at rate ρ_j , detected cases become symptomatic at rate ψ_j , recover naturally at
 123 rate γ_{jq} , or die naturally at rate μ . Symptomatic individuals during the first five days of onset of symptoms are treated
 124 at a rate τ_{j1} and progress to the second infectious class at a rate α_{j1} . These individuals are hospitalized at a rate ϕ_{j1} and
 125 suffer disease-induced death at a rate δ_{j1} . Symptomatic individuals that survived the first five days of onset of symptoms
 126 are treated at a rate τ_{j2} , hospitalized at a rate ϕ_{j2} , recover at a rate γ_{j2} and die of the disease at a rate δ_{j2} . Hospitalized
 127 individuals are treated at a rate τ_{jh} and succumb to the disease at a rate δ_{jh} . Recovered individuals lose the infection-
 128 acquired (natural) immunity, and revert to the wholly-susceptible class, at a rate ω_{jr} .

129 The equations for the transmission dynamics of the two variants of concern (Delta and Omicron) in the United States, in
 130 the presence of vaccination with the FDA-approved Pfizer/BioNTech or Moderna vaccine and treatment of symptomatic
 131 individuals, is given by the following deterministic system of nonlinear differential equations (the flow diagram of the
 132 model is given in Figure 2 and the state variables and parameters of the model are described in Tables S1 and S2 of the
 133 Supplementary Information, respectively):

$$\begin{aligned} \dot{S} &= \Lambda + \omega_{vf}V_f + \omega_{vb}V_b + \omega_{dr}R_d + \omega_{or}R_o - (\lambda_d + \lambda_o + \xi_{vf} + \mu)S, \\ \dot{V}_f &= \xi_{vf}S - (\lambda_{df} + \lambda_{of} + \xi_{vb} + \omega_{vf} + \mu)V_f, \\ \dot{V}_b &= \xi_{vb}V_f - (\lambda_{db} + \lambda_{ob} + \omega_{vb} + \mu)V_b, \\ \dot{E}_j &= \lambda_j S + \lambda_{jf}V_f + \lambda_{jb}V_b - (\sigma_{je} + \rho_j + \mu)E_j, \\ \dot{P}_j &= \sigma_{je}E_j - (\sigma_{jp} + \rho_j + \mu)P_j, \\ \dot{A}_j &= (1 - r_j)\sigma_{jp}P_j - (\gamma_{ja} + \rho_j + \mu)A_j, \\ \dot{Q}_j &= \rho_j(E_j + P_j + A_j) - (\gamma_{jq} + \psi_j + \mu)Q_j, \end{aligned} \quad (2.8)$$

$$\begin{aligned}
 \dot{I}_{j1} &= r_j \sigma_{jp} P_j + \psi_j Q_j - (\tau_{j1} + \alpha_{j1} + \phi_{j1} + \mu + \delta_{j1}) I_{j1}, \\
 \dot{I}_{j2} &= \alpha_{j1} I_{j1} - (\tau_{j2} + \gamma_{j2} + \phi_{j2} + \mu + \delta_{j2}) I_{j2}, \\
 \dot{H}_j &= \phi_{j1} I_{j1} + \phi_{j2} I_{j2} - (\tau_{jh} + \gamma_{jh} + \mu + \delta_{jh}) H_j, \\
 \dot{R}_j &= \gamma_{ja} A_j + \gamma_{jq} Q_j + \tau_{j1} I_{j1} + (\tau_{j2} + \gamma_{j2}) I_{j2} + (\tau_{jh} + \gamma_{jh}) H_j - (\omega_{jr} + \mu) R_j, \text{ with } j \in \{d, o\}.
 \end{aligned}$$

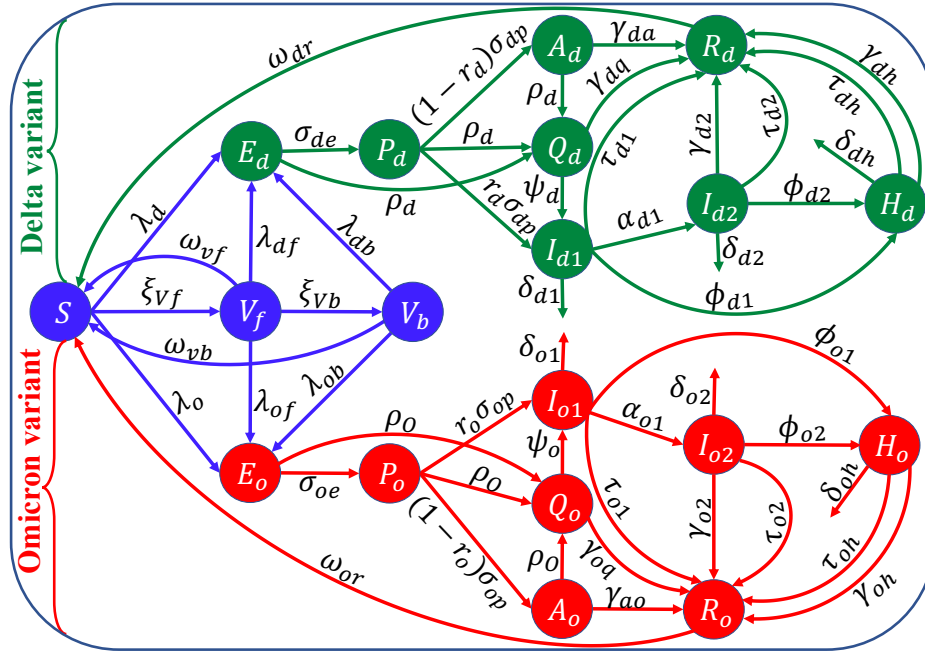


Fig. 2: Flow diagram of the model (2.8). Although recruitment into the population and natural deaths occur (at the rate Λ and μ , respectively), these rates are not illustrated in the flow diagram to make it less crowded and easier to follow. The state variables and parameters are described in Tables S1 and S2 of the Supplementary Information (SI).

134 Some of the main assumptions made in the formulation of the model (2.8) are

- 135 (a) Only the Delta and Omicron variants were co-circulating (i.e., they were the most predominant of all the variants
 136 of concern at the time of this study). Specifically, we consider the scenario where Delta was the dominant strain
 137 and then Omicron emerged (as was the case in the United States during the fall of 2021).
- 138 (b) A well-mixed population, where every individual is equally likely to mix with every other individual in the com-
 139 munity. We also consider an endemic scenario, to account for demographic (birth and natural death) processes.
 140 This is needed to account for the vaccination of children (five years of age and older).
- 141 (c) Vaccines only offer cross-protective efficacy against the variants (since all the FDA-approved vaccines were devel-
 142 oped for the original strain that was circulating in the United States during the early stages of the pandemic).
- 143 (d) Natural immunity and vaccine-derived immunity for fully-vaccinated and boosted humans wane over time.

144 The model (2.8) is an extended version of numerous COVID-19 transmission models in the literature that consider the
 145 dynamics of multiple co-circulating variants, such as those in [46–55] by, *inter alia*, including:

- 146 1. Incorporating a booster dose (this was not considered in [46–55]).
- 147 2. Explicitly modeling the dynamics of the two SARS-CoV-2 variants (Delta and Omicron) that were predominant at
 148 the time this study was carried out and submitted (November 2021 to March 2022).
- 149 3. Incorporating the treatment of symptomatic individuals during and after the first five days of onset of symptoms
 150 (treatment against COVID-19 was not considered in [46–54]). It is worth mentioning that although the agent-based
 151 model considered in Matrajt *et al.* [55] was used to evaluate the impact of treatment on COVID-19 dynamics, the
 152 model does not explicitly account for waning of immunity and the use of a booster shot against the disease.
- 153 4. Allowing for waning vaccine-derived and natural immunity over time (this was not considered in [46–55]).
- 154 5. Explicitly including the impact of voluntary testing to detect infected individuals who do not have clinical symp-
 155 toms of the disease. Although this was not done in [46–55], detection has been incorporated in some models
 156 for COVID-19 dynamics (e.g., [56, 57]). Specifically, the epidemic (SIDARTHE) model developed in [56] consists

of eight epidemiological compartments of Susceptible (S), Infected (I), Diagnosed (D), Ailing (A), Recognized (R), threatened (T), Healed (H) and Extinct (E) individuals, where (in the formulation/notation in [56]) individuals in the I and A compartments are undetected while those in the D , R , and T are detected. Important differences exist between the epidemic SIDARTHE model formulated in [56] and the endemic SVEPAIQRH (Susceptible-Vaccinated-Exposed-Presymptomatic-Asymptomatic-Symptomatic-Detected-Hospitalized-Recovered) model presented in the current study. For instance, the model in [56] did not explicitly include vaccination, births and natural deaths. Furthermore, it assumes that newly-infected individuals are instantaneously capable of transmitting infection (i.e., susceptible individuals move to the I class upon acquisition of infection; this may not be realistic in the context of COVID-19, where infected individuals must first survive either latency (for presymptomatic infectious individuals) or incubation period (for asymptomatic or symptomatic infectious individuals) before they can transmit infection (i.e., before they become infectious).

It should also be stated that detection of infected individuals who do not display clinical symptoms of the disease (i.e., those in the exposed/latent class, E , presymptomatic class, P_j , $j = d, o$, and asymptomatic class, A_j) is crucial in allowing the model to fit the daily confirmed case data reasonably well (we would not get a good model fitting, with respect to the daily confirmed case data if this feature is not included in the model). In particular, including detection of infected individuals in these classes that do not exhibit disease symptoms makes it possible to be able to fit confirmed daily cases in the model to confirmed daily cases from the available data [56].

Finally, although voluntary testing is modeled in our study using constant parameters (τ_{ji} and τ_{jh} , where $j = d, o$, and $i = 1, 2$) (as a first approximation, necessitated by the absence of real data on human behavior with respect to testing in the United States), it may be more appropriate to use time-varying parameters that depend on human behavioral changes to model voluntary testing (as was done in some studies, such as those in [58, 59]).

2.2. Model Fitting and Parameter Estimation

The model (2.8) has several parameters, some of which are known (see Table S3) and some of which are unknown. The key unknown parameters that will be estimated are the effective community transmission rates for infectious individuals in the classes P_d , A_d , Q_d , I_{d1} , I_{d2} , and H_d (i.e., β_{dp} , β_{da} , β_{dq} , β_{d1} , β_{d2} , and β_{dh}), the rate at which individuals are fully-vaccinated (ξ_{vf}), and the rate at which fully-vaccinated individuals are boosted (ξ_{vb}). These parameters will be estimated by fitting the model (2.8) to the confirmed daily COVID-19 case data for the United States for the period from November 28, 2021 to January 31, 2022. The model (2.8) is fitted to (and cross-validated) using the observed data using a standard nonlinear least squares regression model fitting approach [60–62]. Specifically, the fitting and parameter estimation involves computing the best set of parameter values that minimizes the sum of the square difference between the observed new daily confirmed case data and the new daily cases from the model (2.8) (i.e., $\rho_d(E_d + P_d + A_d) + r_d\sigma_{dp}P_d + \rho_o(E_o + P_o + A_o) + r_o\sigma_{op}P_o$). The minimization is implemented in MATLAB version R2021b using the inbuilt “*lsqcurvefit*” algorithm. The 95% confidence intervals for the estimated parameters are determined using a bootstrapping technique [60–62]. Bootstrapping involves producing a large collection of simulated data sets from a given data set by sampling from this given data set with replacement and then using each generated data set to estimate model parameters. These estimations are used for setting confidence intervals based on the distribution of the estimates, which is associated with the actual estimates. In this study, we sample the residuals from the initial parameter estimation using the inbuilt bootstrapping function in MATLAB (“*bootstrap*”) to generate 10,000 bootstrap replicates. The bootstrap data sets are generated by adding the resampled residuals to the best fit curve. The model is then fitted to each bootstrap data set to create the bootstrap distribution of parameter estimates. This distribution is used to estimate the 95% confidence intervals of the parameters via the inbuilt function (“*prctile*”) in MATLAB. Fitting the model to (raw) daily confirmed case data is useful in avoiding mistakes that arise when deterministic models are fitted to cumulative case data [63]. The estimated parameters and the corresponding 95% confidence intervals are tabulated in Table S4.

The results obtained for the fitting of the daily new COVID-19 cases in the United States, for the period when Omicron first emerged (November 28, 2021) until January 31, 2022 (i.e., the region to the left of the dashed vertical black line), is depicted in Figure 3 (a). This figure shows a very good fit between the model output (blue curve) and the observed data (red dots). Furthermore, we show in this figure the prediction of the model for the daily COVID-19 cases for approximately a seven-week period after January 31, 2022 (i.e., for the period from February 1, 2022 to March 18, 2022), as illustrated by the segment of the graph to the right of the dashed vertical black line of Figure 3 (a). This segment of Figure 3 (a) clearly shows that the model (2.8) predicts the observed data for the period from February 1, 2022 to March 18, 2022 perfectly (solid green curve). The model was then simulated (using the fixed and fitted parameter baseline values in Tables S3 and S4) and compared with the observed cumulative case data. The results obtained, depicted in Figure 3 (b), show a very good fit. Furthermore, this figure shows a perfect model prediction for the period from February 1, 2022 to March 18, 2022 (see region to the right of the dashed vertical black line).

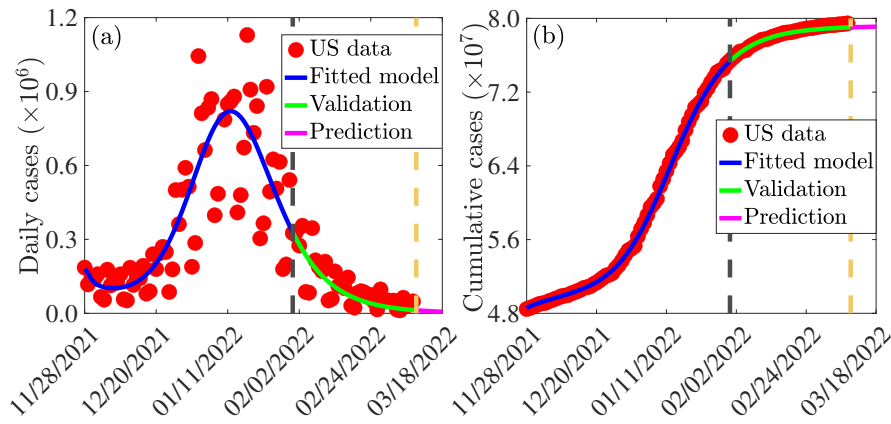


Fig. 3: (a) Time series illustration of the least squares fit of the model (2.8), showing the model's output for the daily cases (blue curve) compared to the observed daily confirmed cases for the United States (red dots) from November 28, 2021 to January 31, 2022 (segment to the left of the dashed vertical black line). (b) Simulation result of the model (2.8), showing cumulative COVID-19 cases for the United States as a function of time, using the fixed and estimated baseline parameter values given in Tables S3 and S4. The segment from February 1, 2022 to March 18, 2022 (i.e., solid green and magenta curves or the entire segment to the right of the dashed black vertical line) illustrates the performance of the model (2.8) in predicting the daily and cumulative cases in the United States.

211 3. Theoretical Analysis

212 In this section, qualitative properties of the model (2.8), with respect to the disease-free equilibrium (DFE), will be ex-
 213 plored. The DFE of the model (2.8) is given by:

$$(S^*, V_f^*, V_b^*, E_d^*, P_d^*, A_d^*, Q_d^*, I_{d1}^*, I_{d2}^*, H_d^*, R_d^*, E_o^*, P_o^*, A_o^*, Q_o^*, I_{o1}^*, I_{o2}^*, H_o^*, R_o^*) = (S^*, V_f^*, V_b^*, 0, 0, 0, 0, 0, 0, 0, 0, 0, 0, 0, 0, 0, 0, 0, 0, 0), \quad (3.1)$$

214 where,

$$S^* = \frac{\Lambda(\omega_{vb} + \mu)(\xi_{vb} + \omega_{vf} + \mu)}{[(\xi_{vb} + \xi_{vf} + \omega_{vf} + \mu)(\omega_{vb} + \mu) + \xi_{vb}\xi_{vf}]\mu}, \quad V_f^* = \frac{\xi_{vf}}{\xi_{vb} + \omega_{vf} + \mu} S^*, \quad V_b^* = \frac{\xi_{vb}\xi_{vf}}{(\omega_{vb} + \mu)(\xi_{vb} + \omega_{vf} + \mu)} S^*.$$

215 3.1. Asymptotic Stability of DFE

216 3.1.1. Local asymptotic stability of DFE

217 The *vaccination reproduction number* of the model, with respect to variant j (with $j \in \{d, o\}$), denoted by \mathbb{R}_{jv} , can be
 218 obtained using the *next generation operator method* [64, 65]. It is given by the following expression:

$$\mathbb{R}_{jv} = \mathbb{R}_{jp} + \mathbb{R}_{ja} + \mathbb{R}_{jq} + \mathbb{R}_{j1} + \mathbb{R}_{j2} + \mathbb{R}_{jh}, \quad (3.2)$$

219 where,

$$\begin{aligned} \mathbb{R}_{jp} &= \frac{\beta_{jp}\sigma_{je}G_{j1}G_{j2}G_{ja}G_{jq}G_{jh}}{G_{je}G_{jp}G_{ja}G_{jq}G_{j1}G_{j2}G_{jh}} H^*, & \mathbb{R}_{ja} &= \frac{\beta_{ja}\sigma_{je}\sigma_{jp}G_{jq}G_{j1}G_{j2}G_{jh}(1-r_j)}{G_{je}G_{jp}G_{ja}G_{jq}G_{j1}G_{j2}G_{jh}} H^*, \\ \mathbb{R}_{jq} &= \frac{\beta_{jq}G_{j1}G_{j2}G_{jh}\rho_j\{[G_{ja} + (1-r_j)\sigma_{jp}]\sigma_{je} + G_{ja}G_{jp}\}}{G_{je}G_{jp}G_{ja}G_{jq}G_{j1}G_{j2}G_{jh}} H^*, \\ \mathbb{R}_{j1} &= \frac{\beta_{j1}G_{j2}G_{jh}\{\{[G_{ja} + (1-r_j)\sigma_{jp}]\psi_j\rho_j + r_j\sigma_{jp}G_{ja}G_{jq}\}\sigma_{je} + \psi_j\rho_jG_{ja}G_{jp}\}}{G_{je}G_{jp}G_{ja}G_{jq}G_{j1}G_{j2}G_{jh}} H^* \\ \mathbb{R}_{j2} &= \frac{\beta_{j2}G_{jh}\alpha_{j1}\{\{[G_{ja} + (1-r_j)\sigma_{jp}]\psi_j\rho_j + r_j\sigma_{jp}G_{ja}G_{jq}\}\sigma_{je} + \psi_j\rho_jG_{ja}G_{jp}\}}{G_{je}G_{jp}G_{ja}G_{jq}G_{j1}G_{j2}G_{jh}} H^*, \\ \mathbb{R}_{jh} &= \frac{\beta_{jh}(\phi_{j1}G_{j2} + \phi_{j2}\alpha_{j1})\{\{[G_{ja} + (1-r_j)\sigma_{jp}]\psi_j\rho_j + r_j\sigma_{jp}G_{ja}G_{jq}\}\sigma_{je} + \psi_j\rho_jG_{ja}G_{jp}\}}{G_{je}G_{jp}G_{ja}G_{jq}G_{j1}G_{j2}G_{jh}} H^*, \end{aligned} \quad (3.3)$$

220 with,

$$H^* = \frac{[S^* + (1 - \varepsilon_{jf})V_f^* + (1 - \varepsilon_{jb})V_b^*]}{S^* + V_f^* + V_b^*}.$$

In (3.3), $G_{je} = \sigma_{je} + \rho_j + \mu$, $G_{jp} = \sigma_{jp} + \rho_j + \mu$, $G_{ja} = \gamma_{ja} + \rho_j + \mu$, $G_{jq} = \gamma_{jq} + \psi_j + \mu$; $G_{j1} = \tau_{j1} + \alpha_{j1} + \phi_{j1} + \mu + \delta_{j1}$, $G_{j2} = \tau_{j2} + \gamma_{j2} + \phi_{j2} + \mu + \delta_{j2}$ and $G_{jh} = \gamma_{jh} + \tau_{jh} + \mu + \delta_{jh}$. It is convenient to define:

$$\mathbb{R}_c = \max\{\mathbb{R}_{dv}, \mathbb{R}_{ov}\}. \quad (3.4)$$

The quantity \mathbb{R}_c is the *vaccination reproduction number* of the model (2.8). It measures the average number of new SARS-CoV-2 cases generated by a typical infectious individual introduced in a community where a certain proportion of the susceptible individuals is fully-vaccinated. The result below follows from Theorem 2 of [65].

Theorem 3.1. *The DFE of the model (2.8) is locally-asymptotically stable if $\mathbb{R}_c < 1$, and unstable if $\mathbb{R}_c > 1$.*

The epidemiological implication of Theorem 3.1 is that a small influx of infected individuals will not generate a large outbreak of the SARS-CoV-2 virus in the community. Thus, the SARS-CoV-2 pandemic can be controlled effectively if the control reproduction number of the model (\mathbb{R}_c) can be brought to a value less than one (and maintained), provided the initial number of infected individuals is small enough. Mathematically-speaking, although bringing \mathbb{R}_c to a value less than one is necessary for elimination of the SARS-CoV-2 virus, it may not be sufficient (owing to the possible existence of a stable endemic equilibrium when $\mathbb{R}_c < 1$, which is well-known to occur for disease transmission models with imperfect vaccines [66–68]). For effective control or elimination of the SARS-CoV-2 virus pandemic to be independent of the initial sizes of the sub-populations of the model, it is crucial to show that the disease-free equilibrium of the model (2.8) is globally-asymptotically stable. This is done, for a special case of the model, in Section 3.1.2 below.

3.1.2. Global asymptotic stability of DFE: special case

Here, the global asymptotic stability of the disease-free equilibrium of the model will be explored for a special case. Consider a special case of the model (2.8) with negligible disease-induced mortality (i.e., $\delta_{j1} = \delta_{j2} = \delta_{jh} = 0$, for $j \in \{d, o\}$) and no waning of vaccine-derived protective immunity for fully-vaccinated (but not boosted) individuals (i.e., $\omega_{vf} = 0$) and no waning of natural immunity (i.e., $\omega_{dr} = \omega_{or} = 0$). Assuming negligible disease-induced mortality is reasonable since at the time of writing, the Omicron variant (which has been the dominant SARS-CoV-2 variant circulating in the United States since its emergence in the fall of 2021), although highly transmissible, was very marginally fatal, in comparison to Delta or any of the other SARS-CoV-2 variants that emerged in the United States [69–72]. The assumptions on waning immunity are made for mathematical tractability. Consider the following feasible region for the model (2.8):

$$\Omega_* = \left\{ (S, V_f, V_b, E_d, P_d, A_d, Q_d, I_{d1}, I_{d2}, H_d, R_d, E_o, P_o, A_o, Q_o, I_{o1}, I_{o2}, H_o, R_o) \in \mathbb{R}_+^{19} : S \leq S^*, V_f \leq V_f^*, V_b \leq V_b^* \right\}.$$

It can be shown (see Section S3.1 of the SI for the proof) that the region Ω_* is positively-invariant and attracting with respect to the special case of the model (2.8). Furthermore, it is convenient to define the following threshold quantity:

$$\hat{\mathbb{R}}_c = \mathbb{R}_c |_{\delta_{j1}=\delta_{j2}=\delta_{jh}=\omega_{vf}=\omega_{jr}=0, j=d,o}. \quad (3.5)$$

We claim the following result:

Theorem 3.2. *Consider the special case of the model (2.8) in the absence of disease-induced mortality (i.e., $\delta_{j1} = \delta_{j2} = \delta_{jh} = 0$) and no waning of vaccine-derived immunity in fully-vaccinated individuals (i.e., $\omega_{vf} = 0$) and no waning of natural immunity (i.e., $\omega_{dr} = \omega_{or} = 0$). The disease-free equilibrium of the special case of the model (given in Eq. (3.1) with $\omega_{vf} = 0$) is globally-asymptotically stable in Ω_* whenever $\hat{\mathbb{R}}_c < 1$.*

The proof of Theorem 3.2, based on using comparison theorem [73], is given in the SI (Section S3.2). The epidemiological implication of Theorem 3.2 is that, for the special case of the model considered above, the COVID-19 pandemic can be effectively eliminated in the United States if the vaccination strategy implemented can result in bringing (and maintaining) the associated control reproduction number ($\hat{\mathbb{R}}_c$) to a value less than one. Mathematically-speaking, Theorem 3.2 implies that $\hat{\mathbb{R}}_c < 1$ is necessary and sufficient for the elimination of the pandemic in the United States.

It is worth mentioning that, using the baseline values of the fixed and estimated parameters of the model (2.8), given in Tables S3 and S4 (used to generate the fittings in Figure 3), shows that the constituent reproduction numbers for the Delta (\mathbb{R}_{dv}) and Omicron (\mathbb{R}_{ov}) are $\mathbb{R}_{dv} = 0.2782 < 1$ (with 95% confidence interval $\mathbb{R}_{dv} \in (0.1991, 0.5197)$) and $\mathbb{R}_{ov} = 0.9602$ (with 95% confidence interval, $\mathbb{R}_{ov} \in (0.6206, 1.7509)$), so that the overall vaccination reproduction number of the model

261 $(\mathbb{R}_c) = \max\{\mathbb{R}_{dv}, \mathbb{R}_{ov}\} = \mathbb{R}_{ov} = 0.9602$. Similarly, for the aforementioned special case of the model, the associated control
 262 reproduction numbers for the Delta and Omicron variants are given, respectively, by $\hat{\mathbb{R}}_{dv} = 0.1098$ (with 95% confidence
 263 interval $\hat{\mathbb{R}}_{dv} \in (0.0547, 0.2129)$) and $\hat{\mathbb{R}}_{ov} = 0.5140$ (with 95% confidence interval, $\hat{\mathbb{R}}_{ov} \in (0.2254, 0.9725)$). Hence, for the spe-
 264 cial case of the model, the overall vaccination reproduction number ($\hat{\mathbb{R}}_c) = \max\{\hat{\mathbb{R}}_{dv}, \hat{\mathbb{R}}_{ov}\} = \hat{\mathbb{R}}_{ov} = 0.5140$. This suggests
 265 that, based on the data for the COVID-19 dynamics in the United States for the period November 28, 2021 to January 31,
 266 2022, the Delta variant has essentially died out (owing to the very low value of its associated control reproduction number
 267 ($\hat{\mathbb{R}}_{dv} = 0.1098 < 1$)) and that the Omicron variant has displaced the Delta variant (since its control reproduction number
 268 is larger) and become the predominant variant in the United States. Furthermore, since the reproduction number of
 269 Omicron (and, hence, of the model (2.8) itself) is less than one, it follows (from Theorem 3.2 or, equivalently, Theorem
 270 3.3 below) that the Omicron variant may also be dying out if the baseline levels of the COVID-19 control measures being
 271 implemented in the United States (as of March 2022) are maintained. In other words, our analysis and data fitting, using
 272 data (as of March 2022) suggests that the COVID-19 pandemic in the United States may be entering its declining phase,
 273 and that elimination is feasible if baseline levels of the control measures being implemented are maintained.

274 3.2. Computation of Vaccine-derived Herd Immunity Threshold

275 To obtain an expression for the vaccine-derived herd immunity threshold [54, 68, 74], it is instructive to recall that the
 276 basic reproduction number for variant j , denoted by \mathbb{R}_{0j} , with $j \in \{d, o\}$, is obtained from (3.2) by setting $V_f = V_b =$
 277 $\varepsilon_{jf} = \varepsilon_{jb} = 0$. It follows that $\mathbb{R}_{0j} = \mathbb{R}_c|_{V_f=V_b=\varepsilon_{jf}=\varepsilon_{jb}=0}$. Let $f_v = \min\{f_{vf}, f_{vb}\}$ be the proportion of individuals who are
 278 fully-vaccinated only (f_{vf}) and those who are fully-vaccinated and boosted (f_{vb}) at steady-state. Furthermore, let $\varepsilon_{jv} =$
 279 $\min\{\varepsilon_{jf}, \varepsilon_{jb}\}$ be the minimum vaccine efficacy for fully-vaccinated (ε_{jf}) and boosted (ε_{jb}) individuals. Setting $\mathbb{R}_c = 1$ in
 280 (3.4), and solving for f_v , gives the following expression for the vaccine-derived herd immunity threshold for Model (2.8):

$$f_v = \frac{1}{\varepsilon_{jv}} \left(1 - \frac{1}{\mathbb{R}_{0j}} \right) = f_v^c. \quad (3.6)$$

281 It follows from (3.6) that $\mathbb{R}_c < (>) 1$ if $f_v^c > (<) 1$. Thus, vaccine-induced herd immunity can be achieved in the community
 282 (and the disease can be eliminated) if $f_v > f_v^c$. Theorem 3.1 can be written in terms of the herd immunity threshold as:

283 **Theorem 3.3.** *The DFE of Model (2.8) is locally-asymptotically stable if $f_v > f_v^c$ ($\mathbb{R}_c < 1$), and unstable if $f_v < f_v^c$ ($\mathbb{R}_c > 1$).*

284 Using the baseline parameter values in Tables S3 and S4, and the herd immunity threshold expression (3.6) shows that
 285 the value of the vaccine-derived herd immunity threshold for the United States is $f_v^c = 0.68$. Thus, our study shows that
 286 vaccine-derived herd immunity can be achieved in the United States (during the time when both Omicron and Delta
 287 are circulating, with the former being the overwhelming predominant variant) if at least 68% of individuals living in the
 288 United States are fully-vaccinated with either the Pfizer and Moderna vaccine. In line with Theorem 3.3, COVID-19 can
 289 be eliminated in the United States if this level of vaccination coverage is attained. Data from [75, 76] shows that about
 290 64% of the United States population is fully-vaccinated as of February 14, 2022. Hence, our study shows that the United
 291 States can eliminate the pandemic if approximately an additional 4% of unvaccinated individuals or individuals who
 292 have received only one dose of the Pfizer or Moderna vaccine become fully-vaccinated with either of these two vaccines.

293 4. Numerical Simulations

294 The model (2.8) is simulated, using the fixed and fitted baseline parameter values in Tables S3 and S4, to assess the im-
 295 pact of vaccination, boosting of vaccine-derived immunity, testing (and detection of infected individuals with no clinical
 296 symptoms of the disease) and treatment of symptomatic individuals on the dynamics of COVID-19 in the United States.
 297

298 Figure 4 depicts contour plots of the control reproduction number of the model, as a function of the efficacy of the two
 299 vaccines (Pfizer or Moderna) against acquisition of infection with Delta or Omicron (defined as $\varepsilon_v = \min\{\varepsilon_{vf}, \varepsilon_{vb}\}$) and
 300 the fraction of the United States population fully-vaccinated at steady-state (defined as $f_v = \min\{f_{vd}, f_{vo}\}$). For the case
 301 where mask usage in the community is maintained at baseline level, this figure shows a decrease in the reproduction
 302 number with increasing values of the vaccine efficacy and coverage. Specifically, for the case when the cross-protective
 303 vaccine efficacy against the two variants is set at 60%, population-wide vaccine-derived herd immunity (associated with
 304 the reduction of the reproduction number to a value below one) can be achieved if 84% of the United States population
 305 is fully-vaccinated with either the Pfizer or Moderna vaccine (Figure 4(a)). It follows from this contour plot that the herd
 306 immunity requirement reduces to 65% if the vaccines offer 80% cross-protective efficacy against the two variants.

307 Further simulations are carried out for the case where the baseline face mask usage in the community is increased by

308 10%, for various mask types. Figure 4(b) shows that if surgical masks are prioritized, the herd immunity requirement corresponding to 60% (80%) cross-protective vaccine efficacy against the variants now reduces to 80% (60%), in comparison to the 84% (65%) coverage recorded for the case with baseline face mask coverage depicted in Figure 4(a). Furthermore, 309
310
311 if N95 masks are prioritized, the herd immunity requirement corresponding to the cross-protective vaccine efficacy of 60% (80%) further reduces to 77% (58%). In summary, the contour plots in Figure 4(b) and (c) show that the proportion of 312
313 individuals who need to be fully-vaccinated to achieve herd immunity reduces with increasing coverage of masks in the community (from the baseline mask usage), and the level of reduction achieved depends on the quality of the mask used 314
315 (specifically, greater reduction in herd immunity level needed to eliminate the disease is achieved if the high-quality N95 masks are prioritized, in comparison to the scenario where the moderate quality surgical masks are prioritized). 316

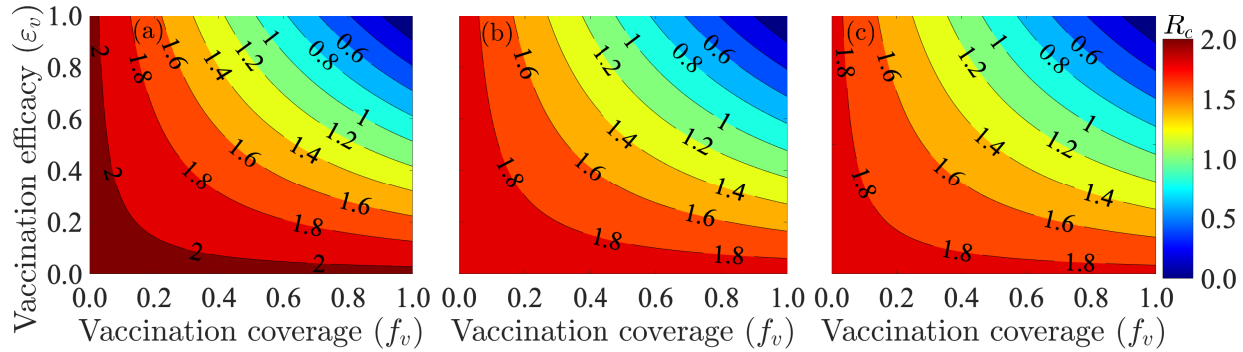


Fig. 4: Contour plots of the control reproduction number of the model (2.8), R_c , as a function vaccine coverage (i.e., proportion of fully-vaccinated individuals, f_v) and cross-protective vaccine efficacy against the variants ($\epsilon_v = \min(\epsilon_{vf}, \epsilon_{vb})$) for the case when (a) mask coverage is maintained at its baseline value, (b) surgical mask is prioritized and the coverage in its usage is increased by 10% from its baseline value, (c) N95 mask is prioritized and the coverage in its usage is increased by 10% from its baseline value. The values of all other parameters used in the simulations are as given by the baseline values in Tables S3 and S4.

317 4.1. Assessing the Impact of Vaccination Coverage

318 The impact of vaccination coverage (i.e., the rate at which unvaccinated susceptible individuals become fully-vaccinated) 319
320 is monitored by simulating the model (2.8) with various values of the vaccination rate (ξ_{vf}). To exclusively monitor 321
322 the impact of vaccination, the simulations are carried out for the special case of the model with no treatment (i.e., all 323
324 treatment-related parameters and state variables of the model are set to zero). The simulation results obtained, depicted in Figure 5, show a significant decrease in the daily (Figure 5 (a)) and cumulative (Figure 5 (b)) COVID-19 cases 325
326 with increasing vaccination coverage of fully-vaccinated individuals (in relation to the baseline value of the vaccination 327
328 coverage), as expected. For instance, this figure shows that increasing the baseline value of the fully-vaccinated rate (ξ_{vf}) 329
330 by 20% resulted in a 12% reduction in daily cases at the peak (Figure 5 (a), gold curve), in comparison to the baseline 331
332 scenario (Figure 5 (a), blue curve). Further reduction (at least 23% at the peak) is achieved if the baseline value of the 333
334 fully-vaccinated vaccination coverage is increased by 40% (Figure 5 (a), green curve). On the other hand, if the baseline 335
336 value of the fully-vaccinated vaccination coverage is decreased, for instance, by 20%, the daily cases at the peak increases 337
338 (compare magenta curve with blue curve of Figure 5 (a)). Similar reductions in cumulative number of cases are recorded 339
340 with increasing fully-vaccinated vaccination coverage rate (Figure 5 (b)). In summary, Figure 5 shows that both the daily 341
342 and cumulative COVID-19 cases can be significantly decreased with even a relatively small increase in the baseline value 343
344 of the fully-vaccinated vaccination rate (e.g., a 20% increase from baseline coverage rate of the fully-vaccinated coverage 345
346 rate). This figure also showed (as of the time of writing in March 2022) that the COVID-19 pandemic can be eliminated 347
348 in the United States, under the baseline vaccination coverage scenario, in late July of 2024. The time-to-elimination is 349
350 accelerated with increasing values of the baseline fully-vaccinated coverage rate. For instance, Figure 5 (a) showed (as 351
352 of the time of writing in March 2022) that elimination can be achieved in June of 2022 if the baseline fully-vaccinated 353
354 coverage rate was increased by 20%.

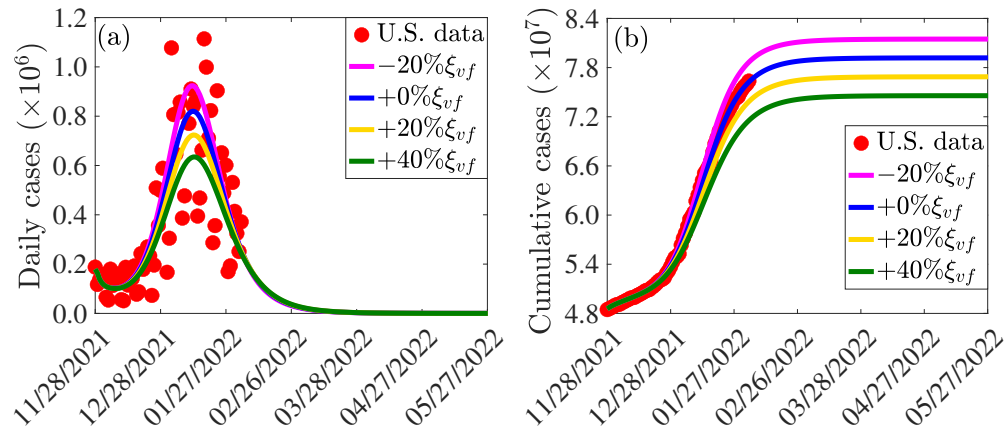


Fig. 5: Simulations of the model (2.8) showing the effect of increases or decreases in fully-vaccinated vaccination coverage rate (ξ_{vf}) on the COVID-19 pandemic in the United States. (a) Daily cases, as a function of time, for various values of the fully-vaccinated vaccination coverage rate. (b) Cumulative cases, as a function of time, for various values of the fully-vaccinated vaccination coverage rate. The values of all other parameters used in these simulations are given by the baseline values in Tables S3 and S4.

338 4.1.1. Assessing the Impact of Additional Increase in Mask Usage from Baseline

339 The incremental impact of masking coverage (and type) on the effectiveness of the vaccination program (here, too, no
 340 treatment of symptomatic individuals is allowed). The simulations are carried out using baseline values of the param-
 341 eters in Tables S3 and S4, with various values of mask coverage (c_m) and types: cloth masks, with estimated efficacy of 30%
 342 (i.e., $\varepsilon_m = 0.3$); surgical masks, with estimated efficacy of 70% (i.e., $\varepsilon_m = 0.7$); and N95 masks, with estimated efficacy of
 343 95% (i.e., $\varepsilon_m = 0.95$). The results obtained, depicted in Figure 6, show that, for the fully-vaccinated vaccination coverage
 344 (using Pfizer/Moderna vaccine) maintained at the baseline value, increasing coverage of mask usage in the community
 345 (c_m) resulted in a dramatic reduction in daily COVID-19 cases, particularly if the moderately-effective surgical or the
 346 highly-effective N95 masks are prioritized (Figure 6 (a)). For example, under this scenario (with fully-vaccinated vac-
 347 cination coverage kept at baseline), a 10% increase in mask coverage with surgical mask (Figure 6 (a), dashed gold curve)
 348 or N95 respirator (Figure 6 (a), dashed green curve) will result in a 26% and 35% decrease in peak daily cases, respectively,
 349 in comparison to the baseline (Figure 6 (a), blue curve). Further reductions are recorded if the coverages of the two mask
 350 types are increased by 20% (Figure 6 (a), solid gold and solid green curves). For the case where only the ineffective cloth
 351 masks are priorities, a 10% increase in baseline coverage of these masks (Figure 6 (a), dashed magenta curve) will result
 352 in approximately 11% decrease in daily cases at the peak, in comparison to the baseline. A further increase to 20% cov-
 353 erage from baseline will result in a 22% decrease in the peak daily cases at baseline (Figure 6 (a), solid magenta curve).
 354 Finally, similar reductions in cumulative cases are also recorded with increasing values of the baseline coverage of each
 355 of the mask type used in the community (Figure 6 (b)).

356 It should be noted that, in all of the simulations carried out in this subsection (and with the same increase in mask
 357 coverage, c_m), greater reductions are recorded using N95 masks, followed by surgical mask, and then cloth masks (as
 358 expected). Furthermore, our results show that a 20% increase in the baseline value of surgical mask coverage (Figures
 359 6 (a)-(b), solid gold curve) is more effective (in reducing cases) than a 10% increase in baseline N95 coverage (Figures
 360 6 (a)-(b), dashed green curve). In other words, our simulations show that, having more people wear the moderately-
 361 effective surgical mask is more effective than having fewer people wear the highly-effective N95 masks. However, this
 362 result, which is consistent with that reported in [77] does not hold when N95 or surgical mask is compared with the low-
 363 effective cloth mask. Specifically, a 20% increase in the baseline coverage of cloth mask (Figures 6 (a)-(b), solid magenta
 364 curve) is not more effective than a 10% increase in the baseline coverage of either surgical (Figures 6 (a)-(b), dashed gold
 365 curve) or N95 (Figures 6 (a)-(b), dashed green curve) mask.

366 Finally, it should be mentioned that relaxing mask usage from the current baseline (as is currently the case in some ju-
 367 risdictions in the United States partially or fully relaxing mask mandates [78–82]) will result in a re-bounce in disease
 368 burden. For example, for the case where mask coverage is decreased by 10% from the current baseline level, our simu-
 369 lations show that a 4-5% increase in the peak daily cases will be recorded if either the surgical mask (Figure 6(c), dashed
 370 purple curve) or N95 mask (6(c), solid magenta curve) is prioritized. Similar increases in the cumulative COVID-19 cases
 371 are recorded with a decrease in baseline coverage of each of the mask type used in the community (Figure 6 (d)). Thus,
 372 our simulations show that, based on the current data and baseline levels of COVID-19 interventions implemented in
 373 the United States, relaxing mask mandates will result in increase in new cases (up to about 5% if surgical or N95 are pri-

374 oritized). Furthermore, giving up masking with surgical mask by a certain proportion is less detrimental than giving up
 375 masking with N95 mask by the same proportion (in other words, reducing coverage of surgical mask by 10%, for instance,
 376 is less detrimental to the community than reducing the coverage of N95 mask by 10%). This figure also shows that fewer
 377 people giving up N95 masks (e.g., 5%) is less detrimental than more people (e.g., 10%) giving up surgical masks.

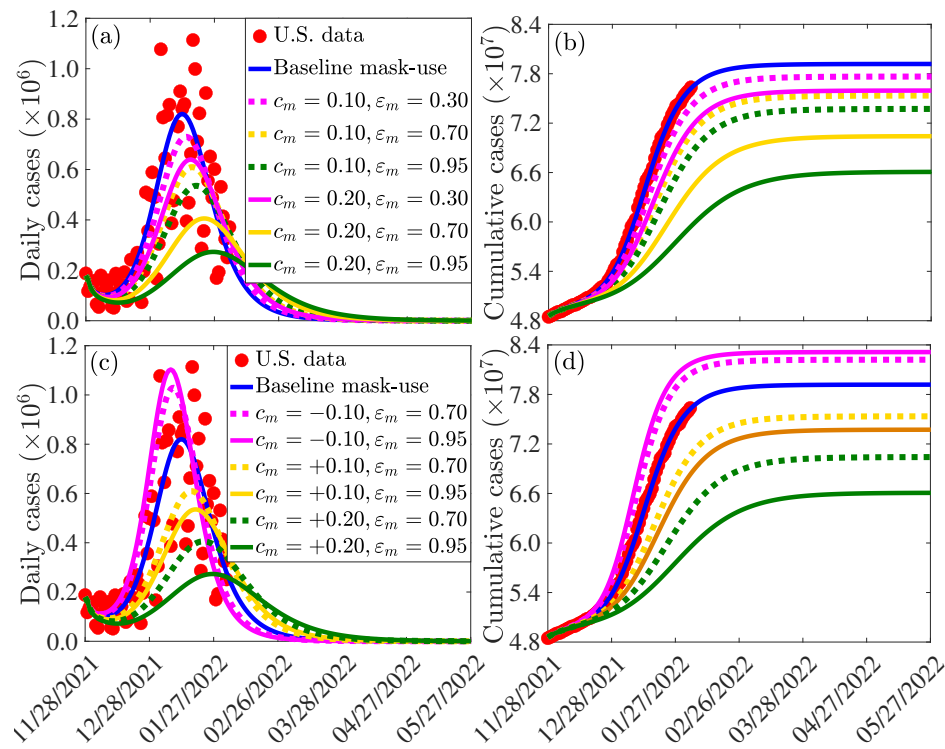


Fig. 6: Simulations of the model (2.8) showing the incremental impact of mask coverage (c_m) and mask type (cloth masks, with $\varepsilon_m = 0.3$; surgical masks, with $\varepsilon_m = 0.7$; and N95 respirators, with $\varepsilon_m = 0.95$) on the daily ((a) and (c)) and cumulative ((b) and (d)) COVID-19 cases in the United States, as a function of time. The values of the other parameters used in these simulations are as given in Tables S3 and S4.

378 In summary, the simulations in this subsection show that, for the case where fully-vaccinated vaccination coverage is
 379 maintained at baseline level (and no treatment strategy is implemented), increasing the baseline value of mask cover-
 380 age reduces the daily and cumulative COVID-19 cases, and the level of reduction increases with increasing quality of the
 381 mask type that is prioritized in the community. For communities that prioritize the use of the moderately-effective sur-
 382 gical and the highly-effective N95 masks only (i.e., communities that discourage the use of cloth masks, which are known
 383 to be generally ineffective [83–86]), having more people (e.g., 20% increase from baseline level) wear surgical masks is
 384 more beneficial to the community than having fewer people (e.g., 10% increase from baseline) wear N95 masks. In other
 385 words, in this context (with only surgical and N95 masks available), significant increase in the coverage of surgical masks
 386 (from their baseline level) may be more effective than a small increase in the baseline coverage of N95 masks.

387 4.1.2. Assessing the Combined Impact of Vaccination and Mask Usage

388 The model (2.8) is further simulated to assess the combined impacts of mask coverage (c_m), mask type (cloth masks,
 389 with $\varepsilon_m = 0.3$; surgical masks, with $\varepsilon_m = 0.7$; and N95 respirators, with $\varepsilon_m = 0.95$) and fully-vaccinated vaccination
 390 coverage rate (ξ_{vf}) on the daily and cumulative number of COVID-19 cases in the United States. For these simulations,
 391 we consider a 20% increase in the baseline values of both mask coverage (c_m) and fully-vaccinated vaccination cover-
 392 age rate (ξ_{vf}). The results obtained, depicted in Figure 7, show that using the ineffective cloth masks will result to a 33%
 393 reduction in the baseline peak daily cases (Figure 7 (a); magenta vs. blue curves). This reduction is better than the 22%
 394 reduction in peak daily cases for the scenario where only the baseline vaccination coverage was increased (Figure 6(a),
 395 solid magenta curve). The reduction in the number of cases is more significant if masks of higher quality are prioritized.
 396 Specifically, if the moderately-effective surgical masks are prioritized, the simulation show that up to 60% reduction in
 397 peak daily cases can be achieved (Figure 7 (a), gold curve). The reduction increases to 74% if the highly-effective N95
 398 masks are prioritized (Figure 7 (a), green curve). These reductions exceed the 51% (67%) reductions recorded, for the
 399 corresponding scenarios, when the fully-vaccinated vaccination coverage was maintained at its baseline value (Figure

400 6 (a), solid gold and green curves). Similar reductions in the cumulative cases are recorded with increasing baseline
 401 vaccination and mask coverage for each of the mask types used in the community (Figure 7 (b)).

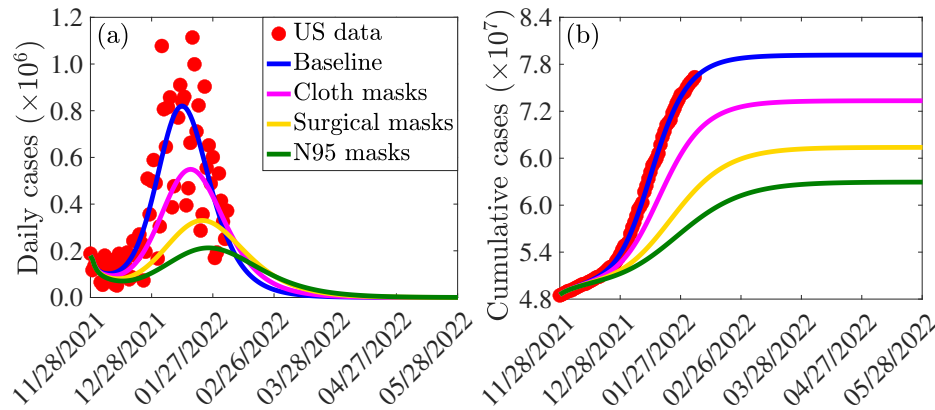


Fig. 7: Simulations of the model (2.8), showing the combined incremental impact of mask coverage (c_m), mask type (cloth masks, with $\varepsilon_m = 0.3$; surgical masks, with $\varepsilon_m = 0.7$; and N95 respirators, with $\varepsilon_m = 0.95$) and fully-vaccinated vaccination coverage rate (ξ_{vf}) on the daily ((a)) and cumulative ((b)) COVID-19 cases in the United States, as a function of time. In these simulations, the mask and fully-vaccinated vaccination coverage rates are increased by 20% from their respective baseline values. The values of the other parameters used in the simulations are given in Tables S3 and S4.

402 Contour plots of the control reproduction number (\mathbb{R}_c) of the model (2.8), as a function of the vaccine rate coverage
 403 (ξ_{vf}) and additional mask coverage (c_m) for different mask types, are generated to determine the optimal combinations
 404 of the mask and vaccination coverage that can reduce the reproduction number to a value less than unity (so that the
 405 pandemic can be eliminated). The results obtained, depicted in Figure S1 in the SI, show that, for a community that
 406 prioritizes surgical masks (and the coverage in its usage is held at baseline), the reproduction number can be brought
 407 down to a value less than unity if up to 798,000 individuals become fully-vaccinated *per day* (i.e., if the fully-vaccinated
 408 vaccination rate is $\xi_{vf} = 0.00532$ *per day*; it should be clarified that the number of fully-vaccinated individuals each day
 409 is given by $\xi_{vf} S$). If the baseline coverage of the surgical mask is increased by 20%, the reproduction number can be
 410 brought to a value less than one if 546,000 individuals are fully-vaccinated each day (i.e., if $\xi_{vf} = 0.00364$). However,
 411 if surgical mask coverage can be increased by 50% from its baseline level, only about 220,500 individuals need to be
 412 fully-vaccinated *per day* to bring the reproduction number to a value less than one. On the other hand, if N95 masks are
 413 prioritized, the requirement for high daily vaccination rate decreases. For instance, if the N95 coverage is increased by
 414 20% from its baseline, only about 462,000 individuals need to be fully-vaccinated every day to bring the reproduction
 415 number to a value less than one (i.e., we need $\xi_{vf} = 0.00308$ *per day*, under this scenario). If the baseline coverage of
 416 N95 in the community can be increased by 50%, the number of individuals that need to be fully-vaccinated everyday
 417 to reduce the reproduction number below one dramatically reduces to 49,500 (i.e., $\xi_{vf} = 0.00033$ *per day* in this case).
 418 In summary, the contour plots in Figure S1 show that the prospects of eliminating COVID-19 in the United States is
 419 more promising if increases in baseline levels of fully-vaccinated vaccination coverage are combined with increases in
 420 baseline levels of face mask coverage that prioritizes moderate (surgical) or high quality (N95) masks.

4.2. Assessing the Impact of Waning of Vaccine-derived and Natural Immunity

422 In this section, the model (2.8) is simulated to assess the effect of waning vaccine-derived and natural immunity on the
 423 dynamics of the SARS-CoV-2 pandemic in the United States. We first considered the case where only the waning rate
 424 of vaccine-derived immunity (for both fully-vaccinated and boosted individuals) varies from its baseline value, while
 425 the waning rate of natural immunity remains at its baseline value (of 9 months). If vaccine-derived immunity wanes
 426 within 3 months (i.e., $\omega_v = \omega_{vf} = \omega_{vb} = 1/(0.25 \times 365) = 0.011$ *per day*), our simulations show that the peak daily cases
 427 increases by 8%, in comparison to the case where vaccine-derived immunity wanes at the baseline value of 9 months
 428 (Figure 8 (a), magenta curve, in comparison to blue curve). A lower peak of the daily cases is recorded if vaccine-derived
 429 immunity wanes in 6 months (Figure 8 (a), gold curve, in comparison to blue curve). If, on the other hand, it takes 4
 430 years for vaccine-derived immunity to wane, our simulations show a marginal decrease in the peak daily cases (about
 431 4% decrease), in comparison to the baseline (Figure 8 (a), green curve, in comparison to blue curve). Similar trends
 432 are observed if only waning natural immunity is varied, while the waning rates of vaccine-derived immunity (for both
 433 fully-vaccinated and boosted individuals) are maintained at their baseline values (Figure 8 (b)) and when both vaccine-
 434 derived and natural immunity are varied from their respective baseline values (Figure 8 (c)). Further, same trends are
 435 observed with respect to the cumulative cases for each of the three variable waning rate scenarios (Figures 8 (d)-(f)).

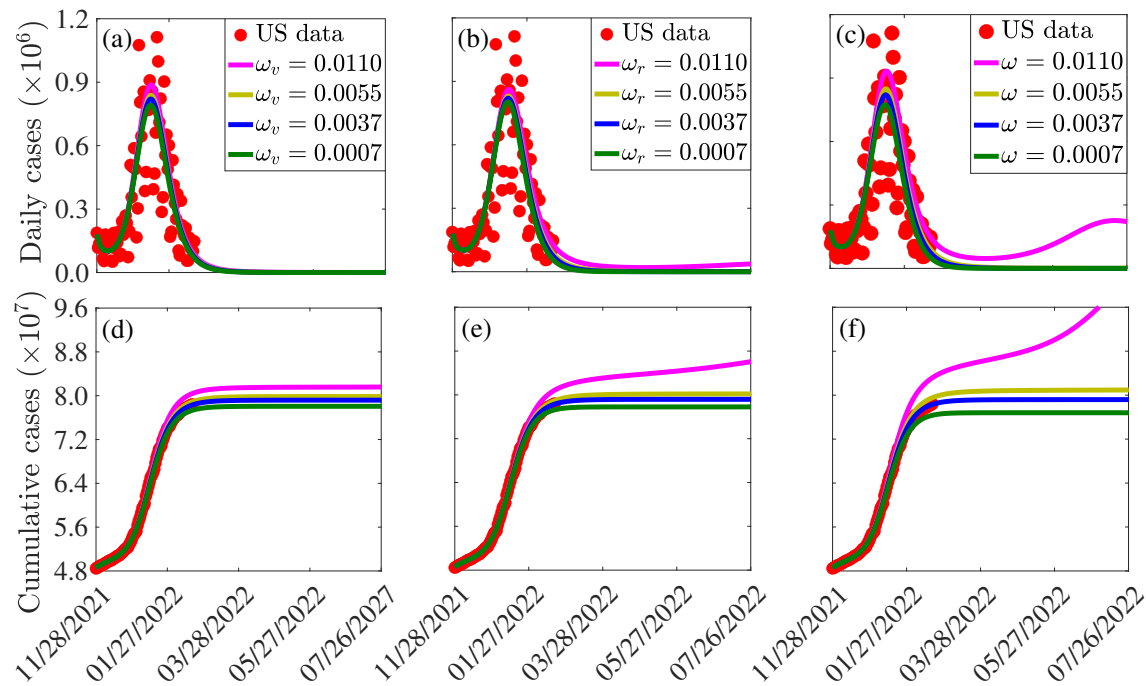


Fig. 8: Simulations of the model (2.8), showing (a)-(c) new daily and (d)-(f) cumulative COVID-19 cases in the United States, as a function of time, for various values of the waning rate of (a) and (d) vaccine-derived immunity in fully-vaccinated and boosted individuals ($\omega_v = \omega_{vf} = \omega_{vb}$), (b) and (e) natural immunity for the Delta and Omicron variants ($\omega_r = \omega_{dr} = \omega_{or}$), and (c) and (f) both vaccine-derived and natural immunity ($\omega = \omega_{vr} = \omega_{vf} = \omega_{vb} = \omega_{dr} = \omega_{or}$). The durations for the waning of immunity were taken to be 3 months (i.e., $\omega = 0.0110$ per day), 6 months ($\omega = 0.0055$ per day), 9 months ($\omega = 0.0037$ per day) and 48 months ($\omega = 0.0007$ per day), respectively. The values of the other parameters used in these simulations are as given in Tables S3-S4.

436 It is worth mentioning that it can be seen from the simulations depicted in Figure 8 that the increase or decrease in
 437 disease burden (i.e., daily or cumulative cases) recorded when the waning rates of both the vaccine-derived and natural
 438 immunity are varied exceed that for the scenario where only the vaccine-derived or the natural immunity is allowed
 439 to vary from baseline. In particular, for the case where both the vaccine-derived and natural immunity wane within
 440 3 months (i.e., $\omega = \omega_{vf} = \omega_{vb} = \omega_{dr} = \omega_{or} = 0.0110$ per day), a 14% increase in the peak new daily cases is recorded, in
 441 comparison to the baseline (we record 8% increase when only vaccine-derived immunity is allowed to vary, as mentioned
 442 above). Furthermore, for this case, our simulations suggest (as of the time of writing in March 2022) that another wave
 443 of the pandemic that peaks by mid July 2022 (with peak new daily cases about 72% lower than those for the baseline
 444 scenario) is predicted to occur (Figure 8 (c), magenta curve). It should, however, be stressed that the simulations in
 445 Figure 8 suggest that decreasing waning rate of the vaccine-derived immunity (up to about 4 years) seems to have only a
 446 marginal impact in decreasing COVID-19 cases. This may be due to the fact that the two vaccines (Pfizer/Moderna) are
 447 highly efficacious against the original SARS-CoV-2 strain, and also moderately-efficacious in the level of cross-protection
 448 they offer against the Delta and Omicron variants.

449 4.3. Assessing the Impact of Antiviral Treatment Against COVID-19

450 In this section, the model (2.8) is simulated to assess the potential impact of the two antiviral drugs (*Paxlovid* and *Mol-*
 451 *nupiravir*) that received FDA Emergency Use Authorization for use in the United States to treat individuals with clinical
 452 symptoms of COVID-19. As of the time of writing (February 2022), the two antivirals are not widely deployed in the
 453 United States. Consequently, there isn't real data to realistically estimate the treatment rates. It should be recalled that
 454 in the model (2.8), treatment is offered to symptomatic individuals (during the first five days or after the first five days of
 455 onset of symptoms) and hospitalized individuals at rates τ_{jk} (where $j = \{d, o\}$, representing the two variants; and $k = 1, 2$,
 456 representing the two symptomatic compartments I_{j1} and I_{j2}). In the absence of the aforementioned data, our simu-
 457 lations will be carried out for the special case where the treatment rate is the same for each treated compartment (i.e.,
 458 $\tau_{j1} = \tau_{j2} = \tau_{jh} = \tau$, with $j = \{d, o\}$). The simulation results obtained are depicted in Figure 9. This figure shows, first of all,
 459 that treatment seems to only have marginal impact in reducing daily new cases (Figure 9 (a)). For instance, if $\tau = 0.8$ (i.e.,
 460 if symptomatic individuals are offered treatment with any of the two antivirals within $1/0.8 = 1.25$ days on average), the
 461 reduction in daily cases, in comparison to the baseline case is marginal (compare blue and green curves in Figure 9(a)).

462 On the other hand, our simulations show that treatment has a more significant impact on reducing daily hospitalization
463 (Figure 9 (b)). For instance, if it takes an average five days to treat a symptomatic individual (i.e., $\tau = 0.2$), a 37% reduction
464 in the peak hospitalization will be recorded, in comparison to the baseline (Figure 9(b), compare magenta and blue
465 curves). Under this scenario, and with all other intervention-related parameters kept at their baseline values (as of the
466 time of writing in March 2022), it will take until June 30, 2024 before the number of COVID-related hospitalizations can
467 be significantly reduced to a few or no hospitalizations at all.

468 If the treatment rate is increased to $\tau = 0.4$ (i.e., if it takes an average of 2.5 days to treat a symptomatic individual), the
469 reduction in baseline peak hospitalization increases to 55% (Figure 9(b), compare gold and blue curves). In this case
470 (and as of the time of writing in March 2022), zero hospitalization (i.e., as stated above, reducing the number of individuals
471 that are hospitalized with the disease to essentially a few or no cases), can be achieved by June 19, 2024. Finally, the
472 reduction in baseline peak hospitalization increases to 72% if $\tau = 0.8$ (Figure 9(b), compare green and blue curves). For
473 this scenario, zero hospitalization can be achieved by June 6, 2024 (this will be visible if Figure 9 is extended to 2024). In
474 summary, the simulations in this subsection show that while treatment only has marginal impact on reducing number
475 of cases, it does have significant impact in reducing daily hospitalizations. With all other interventions (vaccination and
476 masking) maintained at their baseline values, our simulations show that treatment, even at perhaps the highest possible
477 rate (such as a rate associated with treating symptomatic individuals within a day or two of onset of symptoms) will delay
478 COVID-19 elimination (as measured, in these simulations, in terms of attaining zero hospitalization) until 2024. Such
479 elimination can be achieved by increasing the effectiveness and coverages of vaccination and/or mask usage. In other
480 words, the simulations suggest that, while treatment reduces hospitalization (a highly desirable goal too), the prospect
481 of COVID-19 elimination is enhanced by focusing investments on mask usage and vaccination than on treatment.

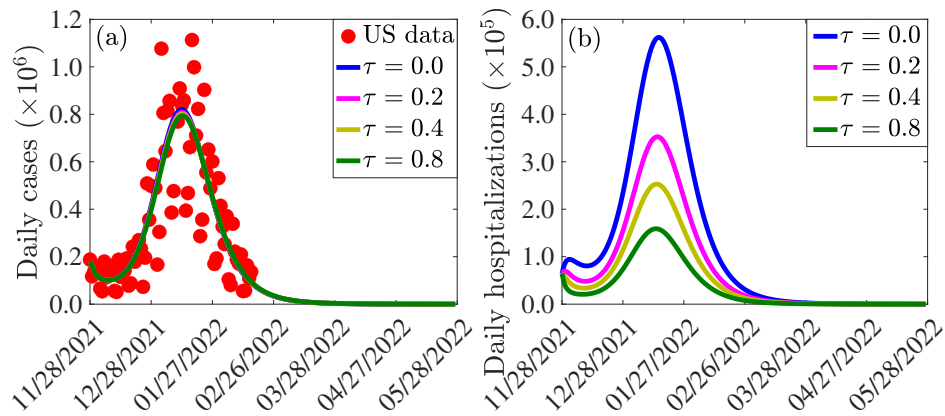


Fig. 9: Simulations of the model (2.8) depicting the impact of treatment of symptomatic infectious and hospitalized individuals on the (a) confirmed daily COVID-19 cases, and (b) daily COVID-19 hospitalizations in the United States. The treatment rate (τ) is given by $\tau = \tau_{j1} = \tau_{j2} = \tau_{jh}$, $j \in \{d, o\}$. The other parameter values used for the simulations are presented in Tables S3 and S4.

482 5. Discussion and Conclusions

483 One of the main success stories in the effort to control the spread of the devastating novel 2019 coronavirus pandemic
484 (COVID-19, caused by SARS-CoV-2) was the rapid development and deployment of safe and effective vaccines [87–90].
485 In particular, the United States Food and Drug Administration (FDA) approved three such vaccines for use in the United
486 States, namely the Pfizer-BioNTech, Moderna and Johnson & Johnson vaccines. Prior to the game-changing moment
487 of the development of these vaccines, control efforts against the SARS-CoV-2 pandemic were limited to the use of non-
488 pharmaceutical interventions, such as quarantine of suspected case, isolation of confirmed cases, use of face masks in
489 public, social-distancing, community lockdowns, etc. Although the vaccines have proven to be very effective in significantly
490 decreasing the burden of the SARS-CoV-2 pandemic in the United States and in other countries and/or regions
491 with moderate to high vaccination coverage (as measured in terms of preventing new cases and minimizing severity of
492 disease, hospitalization and death in breakthrough infections), they have not been able to lead to the elimination of the
493 pandemic. This is largely due to the concerning level of vaccine hesitancy [21, 91–98] and emergence of numerous variants
494 of concern [35–40, 42, 43]. The three vaccines being used in the United States were designed to target the original
495 strain of SARS-CoV-2, and they only offer cross-protective efficacy against the variants that emerged and circulate in the
496 population. The FDA also provided Emergency Use Authorization (EUA) for two very effective antivirals for use to treat

497 individuals with severe symptoms of SARS-CoV-2.

498 Since it is now clear that vaccination alone is insufficient to lead to elimination of the pandemic, it is instructive to
499 develop and use a mathematical modeling framework for assessing the community-wide impact of combining the vac-
500 cination program with other control strategies (NPIs, such as face mask usage, and the two antivirals) in an effort to
501 effectively curtail the COVID-19 pandemic in the United States, and for the scenario where two variants of concern
502 (Delta and Omicron) are co-circulating. This forms the objective of this study. We developed a mathematical model, of
503 the form of a deterministic system of nonlinear differential equations, for assessing the combined impacts of vaccina-
504 tion, face mask usage and antiviral treatment on minimizing and mitigating the burden of the two COVID-19 variants.
505 In our model formulation, vaccination is based on using either the Pfizer or Moderna vaccine (each with protective effi-
506 cacy against acquisition of infection set at about 95%). We fitted and parameterized the model using the observed daily
507 COVID-19 case data for the United States starting from the time when Omicron first emerged (end of November 2021)
508 to the end of January 2022. We then used the additional available data for the period from February 1, 2022 to March
509 10, 2022 for cross validation purpose (i.e., to validate the model). The cross-validation showed that the model perfectly
510 predicts the case data for the time period from February 1, 2022 to March 8, 2022.

511 Qualitative analysis of the model reveals that its disease-free equilibrium is locally-asymptotically stable whenever a cer-
512 tain epidemiological threshold, known as the *control reproduction number* (denoted by \mathbb{R}_c) is less than one. This result
513 is extended to establish the global asymptotic stability of the disease-free equilibrium for a special case of the model.
514 The epidemiological implication of this asymptotic stability result for the disease-free equilibrium of the model is that
515 the SARS-CoV-2 pandemic can be eliminated in the United States if the control measures implemented can bring (and
516 maintain) the reproduction number to a value less than one. The pandemic will persist if the control measures are un-
517 able to bring the control reproduction number to a value less than one.

518 We computed, using the baseline values of the parameters of our model (which was parameterized using observed daily
519 case data for the pandemic in the United States), the value of the threshold quantity \mathbb{R}_c , which is expressed as the max-
520 imum of the constituent reproduction numbers for the spread of the Delta and Omicron variants. This computation
521 showed that, for the simulation period from November 28, 2021 to March 1, 2022, the constituent reproduction number
522 for the Delta variant is 0.28 while that for the Omicron variant is approximately equal to one (0.96). Thus, our study show
523 that Omicron is the predominant variant, and that Delta has essentially died out. Furthermore, if current baseline levels
524 of the control measures implemented in the United States are maintained, Omicron will die out as well (but will persist
525 if the control measures are relaxed, to the extent that the reproduction number for Omicron exceeds one).

526 This study further showed that vaccine-derived herd immunity can be achieved (and the pandemic can be eliminated)
527 if at least 68% of the population is fully-vaccinated with either the Pfizer or Moderna vaccine. Since data from the CDC
528 shows, as of February 14, 2022 that 64% of United States population is already fully-vaccinated [75, 76], our study suggests
529 that increasing the vaccination coverage in the unvaccinated population (and/or population of those who only received
530 one vaccine dose) by about 4% could push the population to achieve herd immunity. If the level of cross-protective
531 immunity offered by the two vaccines against the Delta and Omicron variants is lower than the baseline levels in our
532 simulations (e.g., 60%), the vaccination coverage needed to achieve vaccine-derived herd immunity increases (to 84%).
533

534 We also assessed the impact of combining vaccination with mask usage using various mask types. We showed that the
535 proportion of individuals who need to be fully-vaccinated to achieve herd immunity decreases with increasing coverage
536 of face masks in the community (from the baseline face mask usage), and the level of reduction achieved depends on
537 the quality of the mask used (specifically, a greater reduction in herd immunity level needed to eliminate the disease is
538 achieved if the high-quality N95 masks are prioritized, in comparison to the scenario where moderate quality surgical
539 masks are prioritized). We showed that greater reductions in pandemic burden are recorded using N95 masks, followed
540 by surgical masks, and then cloth masks (as expected). Furthermore, our results show that having more people wear
541 surgical masks is more effective than fewer people wearing N95 masks. This result indicates that the SARS-CoV-2 pan-
542 demic would have been easily controlled if more surgical masks (which are moderately-effective) were made available to
543 the populace during the early stages of the pandemic (since this would have slowed down the spread of the SARS-CoV-2
544 pandemic, while the three safe and effective vaccines authorized for use in the United States were developed).

545 Although the mRNA vaccines (Pfizer, Moderna) designed to fight the original strain of SARS-CoV-2 reduce the risk of hos-
546 pitalization and death and offer some cross protection against variants of concern, the cross protective efficacy they offer
547 wane over time. In particular, the protective efficacy of these vaccines wanes down to about 40% within a few months
548 of the second dose [17, 99, 100]. We simulated the model to assess the impact of waning vaccine-derived immunity (in
549 fully vaccinated and boosted individuals) and natural immunity. Our simulations showed an increase in disease burden
550 if immunity wanes at a faster rate (e.g., if both vaccine-derived and natural immunity wane within 3 months, as against

551 the baseline of within about 9 months to a year), with the possibility of another wave of the Omicron variant (*albeit*
552 much milder one this time, with a projected peak size at least 72% lower than the Omicron peak size recorded in January
553 of 2022). This, and the possibility of future emergence of other SARS-CoV-2 variants of concern (to compete with, or
554 displace, Omicron), suggests that a fourth Pfizer/Moderna booster dose may be needed in the United States this year
555 (2022) to supplement the effort to eliminate the SARS-CoV-2 pandemic. For example, laboratory investigations have
556 suggested that the BA.2 sub-variant of Omicron might lead to more severe disease, and that current vaccines against
557 COVID-19 might not be effective against this sub-variant [101–103]. In any case, our simulation results advocating for
558 a fourth booster dose of Pfizer and Moderna for the United States, is in line with the decision in Israel to authorize a
559 fourth booster dose against the pandemic starting with immuno-compromised individuals, adults over the age of 60
560 and health-care employees, and then adults aged 18 and over [104, 105]. It should be emphasized that our simulations
561 show only a marginal increase in disease burden if both vaccine-derived and natural immunity last at least 6 months.

562 We showed that while the use of the two approved antiviral drugs induce marginal impact in reducing the number of
563 new daily cases of SARS-CoV-2 in the United States, their usage offer a more pronounced effect in reducing hospitaliza-
564 tions. Specifically, if all other interventions (vaccination and masking) are maintained at their baseline values, even the
565 most efficient treatment strategy (e.g., one associated with treating symptomatic cases within a day or two of onset of
566 symptoms) cannot lead to elimination of the COVID-19 pandemic until about the year 2024. However, such elimina-
567 tion can be achieved by increasing the effectiveness and coverages of vaccination and/or mask usage. In other words,
568 our study showed that while treatment reduces hospitalizations, the prospect of COVID-19 elimination is enhanced by
569 focusing investments of control resources on mask usage and vaccination, rather than on treatment options.

570 6. Acknowledgments

571 ABG acknowledges the support, in part, of the Simons Foundation (Award #585022) and the National Science Founda-
572 tion (Grant Number: DMS-2052363). CNN acknowledges the support of the Simons Foundation (Award #627346)
573 and the National Science Foundation (Grant Number: DMS #2151870). HBT acknowledges the support of the Gradu-
574 ate Research Assistantship in Developing Countries Program (from the International Mathematics Union) and Centre
575 d’Excellence Africain en Sciences Mathematiques, Informatique et Applications, Benin. SS acknowledges the support
576 of the Fulbright Foreign Student Program.

577 7. Additional information

578 7.1. Competing interests

579 The author(s) declare no competing interests.

580 7.2. Data availability

581 The data sets used and/or analysed during the current study are available from the websites:

- 582 • <https://github.com/CSSEGISandData/COVID-19>
- 583 • <https://ourworldindata.org/coronavirus/country/united-states>

584 Relevant codes used for analyzing the data and for producing the figures in the paper are uploaded on the appropriate
585 journal platform.

586 References

- 587 [1] D. M. Morens and A. S. Fauci, “The 1918 influenza pandemic: insights for the 21st century,” *The Journal of Infec-*
588 *tious Diseases* **195**, 1018–1028 (2007).
- 589 [2] I. O. Ayenigbara, O. R. Adeleke, G. O. Ayenigbara, J. S. Adegboro, and O. O. Olofintuyi, “COVID-19 (SARS-CoV-2)
590 pandemic: fears, facts and preventive measures,” *Germes* **10**, 218 (2020).
- 591 [3] Q. Li, X. Guan, P. Wu, X. Wang, L. Zhou, Y. Tong, R. Ren, K. S. Leung, E. H. Lau, J. Y. Wong, et al., “Early transmission
592 dynamics in Wuhan, China, of novel coronavirus–infected pneumonia,” *New England Journal of Medicine* (2020).
- 593 [4] C. N. Ngonghala, E. Iboi, S. Eikenberry, M. Scotch, C. R. MacIntyre, M. H. Bonds, and A. B. Gumel, “Mathematical
594 assessment of the impact of non-pharmaceutical interventions on curtailing the 2019 novel coronavirus,” *Math-*
595 *ematical Biosciences* 108364 (2020).

- 596 [5] I. F. Miller, A. D. Becker, B. T. Grenfell, and C. J. E. Metcalf, “Disease and healthcare burden of COVID-19 in the
597 United States,” *Nature Medicine* **26**, 1212–1217 (2020).
- 598 [6] Worldometer., “COVID live update.” Worldometer information (Accessed on February 22, 2022).
599 [Online Version](#)
- 600 [7] E. Dong, H. Du, and L. Gardner, “An interactive web-based dashboard to track COVID-19 in real time,” *The Lancet*
601 *Infectious Diseases* (2020).
- 602 [8] S. M. Moghadas, T. N. Vilches, K. Zhang, C. R. Wells, A. Shoukat, B. H. Singer, L. A. Meyers, K. M. Neuzil, J. M.
603 Langley, M. C. Fitzpatrick, et al., “The impact of vaccination on coronavirus disease 2019 (COVID-19) outbreaks
604 in the United States,” *Clinical Infectious Diseases* **73**, 2257–2264 (2021).
- 605 [9] C. E. Wagner, C. M. Saad-Roy, S. E. Morris, R. E. Baker, M. J. Mina, J. Farrar, E. C. Holmes, O. G. Pybus, A. L. Graham,
606 E. J. Emanuel, et al., “Vaccine nationalism and the dynamics and control of SARS-CoV-2,” *Science* **373**, eabj7364
607 (2021).
- 608 [10] E. Mathieu, H. Ritchie, E. Ortiz-Ospina, M. Roser, J. Hasell, C. Appel, C. Giattino, and L. Rodés-Guirao, “A global
609 database of COVID-19 vaccinations,” *Nature Human Behaviour* **5**, 947–953 (2021).
- 610 [11] Jeff Craven, “COVID-19 vaccine tracker.” Regulator Affairs Professionals Society (RAPS). (Accessed on February
611 22, 2022).
612 [Online Version](#)
- 613 [12] Food and Drugs Administration (FDA), “FDA approves first COVID-19 vaccine,” FDA NEWS Release, 2021 (Ac-
614 cessed on February 16, 2022).
615 [Online Version](#)
- 616 [13] J. H. Tanne, “COVID-19: FDA approves Pfizer-BioNTech vaccine in record time,” (2021).
- 617 [14] Centers for Disease Control and Prevention (CDC), “Different COVID-19 vaccines,” CDC information (Accessed
618 on June 25, 2021).
619 [Online Version](#)
- 620 [15] E. Mahase, “Covid-19: Moderna vaccine is nearly 95% effective, trial involving high risk and elderly people shows,”
621 *BMJ: British Medical Journal (Online)* **371** (2020).
- 622 [16] W. H. Self, M. W. Tenforde, J. P. Rhoads, M. Gaglani, A. A. Ginde, D. J. Douin, S. M. Olson, H. K. Talbot, J. D.
623 Casey, N. M. Mohr, et al., “Comparative effectiveness of Moderna, Pfizer-BioNTech, and Janssen (Johnson &
624 Johnson) vaccines in preventing COVID-19 hospitalizations among adults without immunocompromising con-
625 ditions—United States, March–August 2021,” *Morbidity and Mortality Weekly Report* **70**, 1337 (2021).
- 626 [17] N. Andrews, J. Stowe, F. Kirsebom, S. Toffa, T. Rickeard, E. Gallagher, C. Gower, M. Kall, N. Groves, A.-M. O’Connell,
627 et al., “COVID-19 vaccine effectiveness against the Omicron (B.1.1.529) variant,” *New England Journal of Medicine*
628 **386**, 1532–1546 (2022).
- 629 [18] Centers for Disease Control and Prevention (CDC), “CDC expands eligibility for COVID-19 booster shots to all
630 adults,” CDC information (Accessed on February 22, 2022).
631 [Online Version](#)
- 632 [19] H. S. Sacks, “The single-dose J&J vaccine had 67% efficacy against moderate to severe-critical COVID-19 at ≥ 14
633 d,” *Annals of Internal Medicine* **174**, JC75 (2021).
- 634 [20] Centers for Disease Control and Prevention, “Different COVID-19 vaccines,” CDC information (Accessed on Jan-
635 uary 25, 2021).
636 [Online Version](#)
- 637 [21] V. C. Lucia, A. Kelekar, and N. M. Afonso, “COVID-19 vaccine hesitancy among medical students,” *Journal of Public*
638 *Health* **43**, 445–449 (2021).
- 639 [22] L. J. Abu-Raddad, H. Chemaitelly, and A. A. Butt, “Effectiveness of the BNT162b2 COVID-19 vaccine against the
640 B.1.1.7 and B.1.351 variants,” *New England Journal of Medicine* **385**, 187–189 (2021).

- 641 [23] T. Koyama, D. Weeraratne, J. L. Snowdon, and L. Parida, “Emergence of drift variants that may affect COVID-19
642 vaccine development and antibody treatment,” *Pathogens* **9**, 324 (2020).
- 643 [24] J. S. Tregoning, K. E. Flight, S. L. Higham, Z. Wang, and B. F. Pierce, “Progress of the COVID-19 vaccine effort:
644 viruses, vaccines and variants versus efficacy, effectiveness and escape,” *Nature Reviews Immunology* **21**, 626–
645 636 (2021).
- 646 [25] S. Loomba, A. de Figueiredo, S. J. Piatek, K. de Graaf, and H. J. Larson, “Measuring the impact of COVID-19 vaccine
647 misinformation on vaccination intent in the UK and USA,” *Nature Human Behaviour* **5**, 337–348 (2021).
- 648 [26] E. Dubé, C. Laberge, M. Guay, P. Bramadat, R. Roy, and J. A. Bettinger, “Vaccine hesitancy: an overview,” *Human
649 Vaccines & Immunotherapeutics* **9**, 1763–1773 (2013).
- 650 [27] C. Jarrett, R. Wilson, M. O’Leary, E. Eckersberger, H. J. Larson, et al., “Strategies for addressing vaccine hesitancy—a
651 systematic review,” *Vaccine* **33**, 4180–4190 (2015).
- 652 [28] P. Paterson, F. Meurice, L. R. Stanberry, S. Glismann, S. L. Rosenthal, and H. J. Larson, “Vaccine hesitancy and
653 healthcare providers,” *Vaccine* **34**, 6700–6706 (2016).
- 654 [29] M. Siddiqui, D. A. Salmon, and S. B. Omer, “Epidemiology of vaccine hesitancy in the United States,” *Human
655 Vaccines & Immunotherapeutics* **9**, 2643–2648 (2013).
- 656 [30] N. E. MacDonald et al., “Vaccine hesitancy: Definition, scope and determinants,” *Vaccine* **33**, 4161–4164 (2015).
- 657 [31] The U.S. Food and Drug Administration (FDA), “Coronavirus (COVID-19) update: FDA authorizes additional oral
658 antiviral for treatment of COVID-19 in certain adults,” FDA NEWS RELEASE (Accessed on February 24, 2022).
659 [Online Version](#)
- 660 [32] Pfizer Inc. (NYSE: PFE).(2022)., “Pfizer shares in vitro efficacy of novel COVID-19 oral treatment against Omicron
661 variant,” Pfizer information (Accessed on February 24, 2022).
662 [Online Version](#)
- 663 [33] A. Jayk Bernal, M. M. Gomes da Silva, D. B. Musungaie, E. Kovalchuk, A. Gonzalez, V. Delos Reyes, A. Martín-Quirós,
664 Y. Caraco, A. Williams-Diaz, M. L. Brown, et al., “Molnupiravir for oral treatment of COVID-19 in nonhospitalized
665 patients,” *New England Journal of Medicine* (2021).
- 666 [34] Food and Drugs Administration (FDA), “Coronavirus (COVID-19) update: FDA authorizes first oral antiviral for
667 treatment of COVID-19,” FDA NEWS Release, 2021 (Accessed on February 16, 2022).
668 [Online Version](#)
- 669 [35] E. Mahase, “COVID-19: What new variants are emerging and how are they being investigated?” (2021).
- 670 [36] A. Gómez-Carballa, J. Pardo-Seco, X. Bello, F. Martínón-Torres, and A. Salas, “Superspreading in the emergence of
671 COVID-19 variants,” *Trends in Genetics* **37**, 1069–1080 (2021).
- 672 [37] Centers for Disease Control and Prevention (CDC), “Variant proportions,” CDC information (Accessed on Febru-
673 ary 24, 2022).
674 [Online Version](#)
- 675 [38] S. S. A. Karim and Q. A. Karim, “Omicron SARS-CoV-2 variant: a new chapter in the COVID-19 pandemic,” *The
676 Lancet* **398**, 2126–2128 (2021).
- 677 [39] D. Duong, “What’s important to know about the new COVID-19 variants?” (2021).
- 678 [40] D. Geers, M. C. Shamier, S. Bogers, G. den Hartog, L. Gommers, N. N. Nieuwkoop, K. S. Schmitz, L. C. Rijsber-
679 gen, J. A. van Osch, E. Dijkhuizen, et al., “SARS-CoV-2 variants of concern partially escape humoral but not t cell
680 responses in COVID-19 convalescent donors and vaccine recipients,” *Science Immunology* **6**, eabj1750 (2021).
- 681 [41] P. Mlcochova, S. A. Kemp, M. S. Dhar, G. Papa, B. Meng, I. A. Ferreira, R. Datir, D. A. Collier, A. Albecka, S. Singh,
682 et al., “SARS-CoV-2 B.1.617.2 Delta variant replication and immune evasion,” *Nature* **599**, 114–119 (2021).
- 683 [42] C. Del Rio, S. B. Omer, and P. N. Malani, “Winter of omicron—the evolving COVID-19 pandemic,” *JAMA* (2021).
- 684 [43] E. Callaway, H. Ledford, et al., “How bad is Omicron? what scientists know so far,” *Nature* **600**, 197–199 (2021).

- 685 [44] E. Dong, H. Du, and L. Gardner, “Coronavirus COVID-19 Global Cases by Johns Hopkins CSSE,” *The Lancet Infectious Diseases* (2020).
686 [Online Version](#)
687
- 688 [45] B. J. Gardner and A. M. Kilpatrick, “Estimates of reduced vaccine effectiveness against hospitalization, infection,
689 transmission and symptomatic disease of a new SARS-CoV-2 variant, Omicron (B.1.1.529), using neutralizing anti-
690 body titers,” *MedRxiv* (2021).
- 691 [46] M. Betti, N. Bragazzi, J. Heffernan, J. Kong, and A. Raad, “Could a new COVID-19 mutant strain undermine vacci-
692 nation efforts? a mathematical modelling approach for estimating the spread of b. 1.1. 7 using Ontario, Canada,
693 as a case study,” *Vaccines* **9**, 592 (2021).
- 694 [47] G. Gonzalez-Parra, D. Martínez-Rodríguez, and R. J. Villanueva-Micó, “Impact of a new SARS-CoV-2 variant on the
695 population: A mathematical modeling approach,” *Mathematical and Computational Applications* **26**, 25 (2021).
- 696 [48] M. Mancuso, S. E. Eikenberry, and A. B. Gumel, “Will vaccine-derived protective immunity curtail COVID-19 vari-
697 ants in the US?” *Infectious Disease Modelling* **6**, 1110–1134 (2021).
- 698 [49] O. Alagoz, A. K. Sethi, B. W. Patterson, M. Churpek, G. Alhanea, E. Scaria, and N. Safdar, “The impact of vaccina-
699 tion to control COVID-19 burden in the United States: A simulation modeling approach,” *PloS One* **16**, e0254456
700 (2021).
- 701 [50] A. Shoukat, T. N. Vilches, S. M. Moghadas, P. Sah, E. C. Schneider, J. Shaff, A. Ternier, D. A. Chokshi, and A. P.
702 Galvani, “Lives saved and hospitalizations averted by COVID-19 vaccination in New York City: a modeling study,”
703 *The Lancet Regional Health-Americas* **5**, 100085 (2022).
- 704 [51] J. Roy, S. Heath, D. Ramkrishna, and S. Wang, “Modeling of COVID-19 transmission dynamics on US population:
705 Inter-transfer infection in age groups, mutant variants, and vaccination strategies,” *MedRxiv* (2021).
- 706 [52] A. ul Rehman, R. Singh, and P. Agarwal, “Modeling, analysis and prediction of new variants of COVID-19 and
707 dengue co-infection on complex network,” *Chaos, Solitons & Fractals* **150**, 111008 (2021).
- 708 [53] A. Ramos, M. Vela-Pérez, M. Ferrández, A. Kubik, and B. Ivorra, “Modeling the impact of SARS-CoV-2 variants
709 and vaccines on the spread of COVID-19,” *Communications in Nonlinear Science and Numerical Simulation* **102**,
710 105937 (2021).
- 711 [54] A. B. Gumel, E. A. Iboi, C. N. Ngonghala, and G. A. Ngwa, “Toward achieving a vaccine-derived herd immunity
712 threshold for COVID-19 in the US,” *Frontiers in Public Health* **9** (2021).
- 713 [55] L. Matrajt, E. R. Brown, D. Dimitrov, and H. Janes, “The role of antiviral treatment in curbing the COVID-19 pan-
714 demic: a modeling study,” *MedRxiv* (2021).
- 715 [56] G. Giordano, F. Blanchini, R. Bruno, P. Colaneri, A. Di Filippo, A. Di Matteo, and M. Colaneri, “Modelling the covid-
716 19 epidemic and implementation of population-wide interventions in italy,” *Nature Medicine* **26**, 855–860 (2020).
- 717 [57] C. N. Ngonghala, E. Iboi, and A. B. Gumel, “Could masks curtail the post-lockdown resurgence of COVID-19 in the
718 US?” *Mathematical Biosciences* **329**, 108452 (2020).
- 719 [58] F. Verelst, L. Willem, and P. Beutels, “Behavioural change models for infectious disease transmission: a systematic
720 review (2010–2015),” *Journal of The Royal Society Interface* **13**, 20160820 (2016).
- 721 [59] B. Buonomo and R. Della Marca, “Effects of information-induced behavioural changes during the COVID-19 lock-
722 downs: the case of Italy,” *Royal Society Open Science* **7**, 201635 (2020).
- 723 [60] H. T. Banks, M. Davidian, J. R. Samuels, and K. L. Sutton, *An Inverse Problem Statistical Methodology Summary*,
724 249–302 (Springer Netherlands, Dordrecht, 2009).
725 [Online Version](#)
- 726 [61] G. Chowell, “Fitting dynamic models to epidemic outbreaks with quantified uncertainty: a primer for parameter
727 uncertainty, identifiability, and forecasts,” *Infectious Disease Modelling* **2**, 379–398 (2017).
- 728 [62] C. N. Ngonghala, E. Iboi, S. Eikenberry, M. Scotch, C. R. MacIntyre, M. H. Bonds, and A. B. Gumel, “Mathematical
729 assessment of the impact of non-pharmaceutical interventions on curtailing the 2019 novel coronavirus,” *Math-
730 ematical Biosciences*. **325**, 108364 (2020).

- 731 [63] A. A. King, M. Domenech de Cellès, F. M. Magpantay, and P. Rohani, “Avoidable errors in the modelling of outbreaks
732 of emerging pathogens, with special reference to Ebola,” *Proceedings of the Royal Society B: Biological Sciences*
733 **282**, 20150347 (2015).
- 734 [64] O. Diekmann, J. A. P. Heesterbeek, and J. A. Metz, “On the definition and the computation of the basic reproduction
735 ratio R_0 in models for infectious diseases in heterogeneous populations,” *Journal of Mathematical Biology* **28**,
736 365–382 (1990).
- 737 [65] P. van den Driessche and J. Watmough, “Reproduction numbers and sub-threshold endemic equilibria for com-
738 partmental models of disease transmission,” *Mathematical Biosciences* **180**, 29–48 (2002).
- 739 [66] A. Gumel, “Causes of backward bifurcations in some epidemiological models,” *Journal of Mathematical Analysis*
740 *and Applications* **395**, 355–365 (2012).
- 741 [67] B. Buonomo and D. Lacitignola, “Forces of infection allowing for backward bifurcation in an epidemic model with
742 vaccination and treatment,” *Acta Applicandae Mathematicae* **122**, 283–293 (2012).
- 743 [68] A. B. Gumel, E. A. Iboi, C. N. Ngonghala, and E. H. Elbasha, “A primer on using mathematics to understand COVID-
744 19 dynamics: Modeling, analysis and simulations,” *Infectious Disease Modelling* **6**, 148–168 (2021).
- 745 [69] T. Nyberg, N. M. Ferguson, S. G. Nash, H. H. Webster, S. Flaxman, N. Andrews, W. Hinsley, J. L. Bernal, M. Kall,
746 S. Bhatt, et al., “Comparative analysis of the risks of hospitalisation and death associated with SARS-CoV-2 Omicron
747 (B.1.1.529) and delta (B.1.617.2) variants in England: a cohort study,” *The Lancet* **399**, 1303–1312 (2022).
- 748 [70] P. A. Christensen, R. J. Olsen, S. W. Long, R. Snehal, J. J. Davis, M. O. Saavedra, K. Reppond, M. N. Shyer, J. Cambric,
749 R. Gadd, et al., “Signals of significantly increased vaccine breakthrough, decreased hospitalization rates, and less
750 severe disease in patients with Coronavirus disease 2019 caused by the Omicron variant of severe acute respiratory
751 syndrome Coronavirus 2 in Houston, Texas,” *The American Journal of Pathology* **192**, 642–652 (2022).
- 752 [71] A. Fall, R. E. Eldesouki, J. Sachithanandham, C. P. Morris, J. M. Norton, D. C. Gaston, M. Forman, O. Abdul-
753 lah, N. Gallagher, M. Li, et al., “A quick displacement of the SARS-CoV-2 variant Delta with Omicron: unprece-
754 dented spike in COVID-19 cases associated with fewer admissions and comparable upper respiratory viral loads,”
755 *MedRxiv* (2022).
- 756 [72] R. P. Bhattacharyya and W. P. Hanage, “Challenges in inferring intrinsic severity of the SARS-CoV-2 Omicron vari-
757 ant,” *New England Journal of Medicine* **386**, e14 (2022).
- 758 [73] V. Lakshmikantham, S. Leela, and A. A. Martynyuk, *Stability Analysis of Nonlinear Systems* (Springer, 1989).
- 759 [74] E. A. Iboi, C. N. Ngonghala, and A. B. Gumel, “Will an imperfect vaccine curtail the COVID-19 pandemic in the
760 US?” *Infectious Disease Modelling* **5**, 510–524 (2020).
- 761 [75] US Coronavirus vaccine tracker, “What’s the nation’s progress on vaccinations?” USA facts (Accessed on February
762 16, 2022).
763 [Online Version](#)
- 764 [76] Centers for Disease Control and Prevention (CDC), “COVID-19 vaccinations in the United States,” CDC COVID-19
765 data tracker (Accessed on February 16, 2022).
766 [Online Version](#)
- 767 [77] S. E. Eikenberry, M. Muncuso, E. Iboi, T. Phan, E. Kostelich, Y. Kuang, and A. B. Gumel, “To mask or not to mask:
768 Modeling the potential for face mask use by the general public to curtail the COVID-19 pandemic,” *Infectious*
769 *Disease Modeling* **5**, 293–308 (2020).
- 770 [78] P. Hodjat, P. A. Christensen, S. Subedi, D. W. Bernard, R. J. Olsen, and S. W. Long, “The reemergence of seasonal
771 respiratory viruses in Houston, Texas, after relaxing COVID-19 restrictions,” *Microbiology Spectrum* **9**, e00430–21
772 (2021).
- 773 [79] G. P. Guy, G. M. Massetti, and E. Sauber-Schatz, “Mask mandates, on-premises dining, and COVID-19,” *JAMA* **325**,
774 2199–2200 (2021).

- 775 [80] The New York Times, “The U.S. states that are ending mask mandates,” The New York Times (Accessed on February
776 19, 2022).
777 [Online Version](#)
- 778 [81] Y. Avila, B. Harvey, J. C. Lee, and J. W. Shaver, “See mask mandates and guidance in each state,” The New York
779 Times (Accessed on February 19, 2022).
780 [Online Version](#)
- 781 [82] M. Hersher, “Nearly half of state mask mandates have ended in the past 3 weeks,” NBC News (Accessed on Febru-
782 ary 19, 2022).
783 [Online Version](#)
- 784 [83] NIOSH, “42 CFR 84 respiratory protective devices; final rules and notice. US Centers for Disease Control and Pre-
785 vention, National Institute for Occupational Safety and Health,” Federal Register **60**, 110 (1997).
- 786 [84] N. H. Leung, D. K. Chu, E. Y. Shiu, K.-H. Chan, J. J. McDevitt, B. J. Hau, H.-L. Yen, Y. Li, D. K. Ip, J. Peiris, et al.,
787 “Respiratory virus shedding in exhaled breath and efficacy of face masks,” *Nature Medicine* **26**, 676–680 (2020).
- 788 [85] Centers for Disease Control and Prevention, “NIOSH-approved particulate filtering facepiece respirators,” The
789 National Personal Protective Technology Laboratory (NPPTL) (Accessed on July 24, 2021).
790 [Online Version](#)
- 791 [86] W. Lindsley, F. Blachere, B. Law, D. Beezhold, and D. John, “Efficacy of face masks, neck gaiters and face shields for
792 reducing the expulsion of simulated cough-generated aerosols,” *Aerosol Science and Technology* **55** (2021).
- 793 [87] N. Lurie, M. Saville, R. Hatchett, and J. Halton, “Developing COVID-19 vaccines at pandemic speed,” *New England*
794 *Journal of Medicine* **382**, 1969–1973 (2020).
- 795 [88] B. S. Graham, “Rapid COVID-19 vaccine development,” *Science* **368**, 945–946 (2020).
- 796 [89] S. Su, L. Du, and S. Jiang, “Learning from the past: development of safe and effective COVID-19 vaccines,” *Nature*
797 *Reviews Microbiology* **19**, 211–219 (2021).
- 798 [90] J. L. Bernal, N. Andrews, C. Gower, E. Gallagher, R. Simmons, S. Thelwall, J. Stowe, E. Tessier, N. Groves, G. Dabrera,
799 et al., “Effectiveness of COVID-19 vaccines against the B.1.617.2 (Delta) variant,” *New England Journal of Medicine*
800 (2021).
- 801 [91] G. Troiano and A. Nardi, “Vaccine hesitancy in the era of COVID-19,” *Public Health* **194**, 245–251 (2021).
- 802 [92] S. Machingaidze and C. S. Wiysonge, “Understanding COVID-19 vaccine hesitancy,” *Nature Medicine* **27**, 1338–
803 1339 (2021).
- 804 [93] A. A. Dror, N. Eisenbach, S. Taiber, N. G. Morozov, M. Mizrahi, A. Zigran, S. Srouji, and E. Sela, “Vaccine hesitancy:
805 the next challenge in the fight against COVID-19,” *European Journal of Epidemiology* **35**, 775–779 (2020).
- 806 [94] P. Soares, J. V. Rocha, M. Moniz, A. Gama, P. A. Lares, A. R. Pedro, S. Dias, A. Leite, and C. Nunes, “Factors associated
807 with COVID-19 vaccine hesitancy,” *Vaccines* **9**, 300 (2021).
- 808 [95] A. Coustasse, C. Kimble, and K. Maxik, “COVID-19 and vaccine hesitancy: a challenge the United States must
809 overcome,” *The Journal of Ambulatory Care Management* **44**, 71–75 (2021).
- 810 [96] A. Fridman, R. Gershon, and A. Gneezy, “COVID-19 and vaccine hesitancy: A longitudinal study,” *PloS One* **16**,
811 e0250123 (2021).
- 812 [97] J. Murphy, F. Vallières, R. P. Bentall, M. Shevlin, O. McBride, T. K. Hartman, R. McKay, K. Bennett, L. Mason,
813 J. Gibson-Miller, et al., “Psychological characteristics associated with COVID-19 vaccine hesitancy and resistance
814 in Ireland and the United Kingdom,” *Nature Communications* **12**, 1–15 (2021).
- 815 [98] M. Sallam, “COVID-19 vaccine hesitancy worldwide: a concise systematic review of vaccine acceptance rates,”
816 *Vaccines* **9**, 160 (2021).
- 817 [99] H. F. Tseng, B. K. Ackerson, Y. Luo, L. S. Sy, C. Talarico, Y. Tian, K. Bruxvoort, J. E. Tupert, A. Florea, J. H. Ku, et al.,
818 “Effectiveness of mRNA-1273 against SARS-CoV-2 omicron and delta variants,” *MedRxiv* (2022).

- 819 [100] C. Willyard et al., “What the omicron wave is revealing about human immunity,” *Nature* **602**, 22–25 (2022).
- 820 [101] B. Goodman, “As BA.2 subvariant of Omicron rises, lab studies point to signs of severity,” CNN (Accessed on Febru-
821 ary 21, 2022).
822 [Online Version](#)
- 823 [102] D. Yamasoba, I. Kimura, H. Nasser, Y. Morioka, N. Nao, J. Ito, K. Uriu, M. Tsuda, J. Zahradnik, K. Shirakawa, et al.,
824 “Virological characteristics of SARS-CoV-2 BA.2 variant,” *BioRxiv* (2022).
- 825 [103] J. Chen and G.-W. Wei, “Omicron BA. 2 (B. 1.1. 529.2): high potential to becoming the next dominating variant,”
826 *ArXiv Preprint ArXiv:2202.05031* (2022).
- 827 [104] D. Williams, “Israel mulls offering 4th COVID vaccine dose to all adults,” Reuters (Accessed on February 21, 2022).
828 [Online Version](#)
- 829 [105] T. K. Burki, “Fourth dose of COVID-19 vaccines in Israel,” *The Lancet Respiratory Medicine* **10**, e19 (2022).
830 [Online Version](#)
831